1957

Investigation of multi-beam bridges (Progress Report No. 14), Proc. ACI, 29 (6) December 1957, Reprint No. 128 (58-1)

R. E. Walther

PRESTRESSED CONCRETE BRIDGE MEMBERS

PROGRESS REPORT NO. 14

INVESTIGATION OF MULTI-BEAM

BRIDGES

LABORATORY TESTS AND ANALYSIS

RENÉ E. WALTHER

Prestressed Concrete Bridge Members

Progress Report 14

INVESTIGATION OF MULTI-BEAM BRIDGES

Laboratory Tests and Analysis

by

René E. Walther

LEHIGH UNIVERSITY

Fritz Laboratory Report 223.14

August 1956

This work has been carried out at

LEHIGH UNIVERSITY
FRITZ ENGINEERING LABORATORY
DEPARTMENT OF CIVIL ENGINEERING

Director
Professor W. J. Eney

PERSONNEL ENGAGED IN THE TESTS

CHAIRMAN OF THE CONCRETE DIVISION:

DR. CARL E. EKBERG, JR. Associate Professor
of Civil Engineering

PLANNING AND REPORTING THE TESTS:

RENÉ E. WALTHER Research Associate

PERFORMING THE TESTS:

KENNETH R. HARPEL Laboratory Foreman

IVAN J. TAYLOR Instrument Associate

LOUIS J. DEBLY Research Assistant

CHARLES E. STUHLMAN Research Assistant

DONALD G. LEITCH Research Assistant

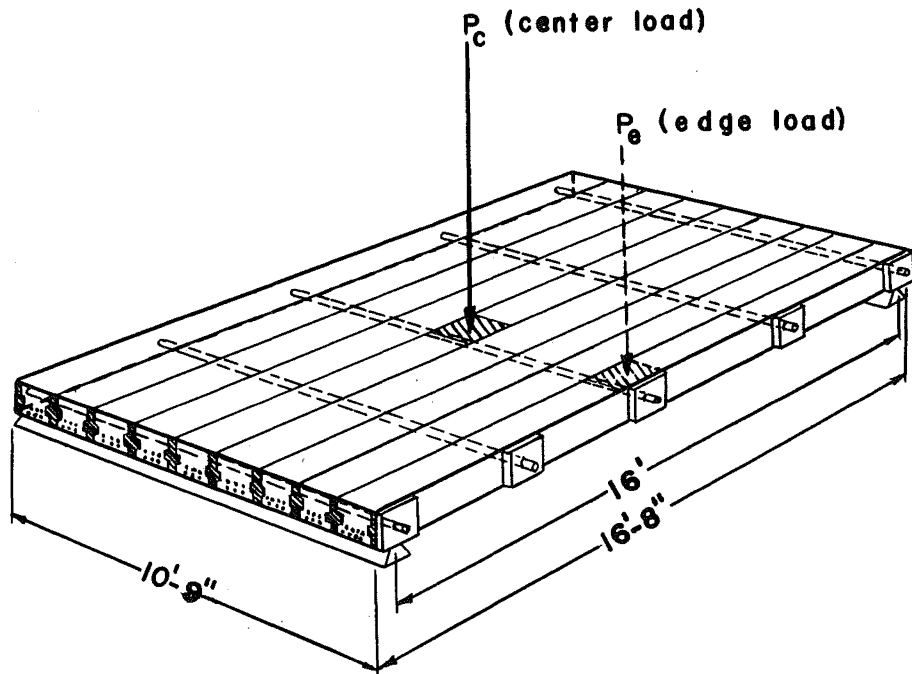ANTONIO M. LOCSIN Research Fellow

DRAFTSMAN:

ALEX W. ADLER

SECRETARY:

MRS. ARLENE WARG

TABLE OF CONTENTS

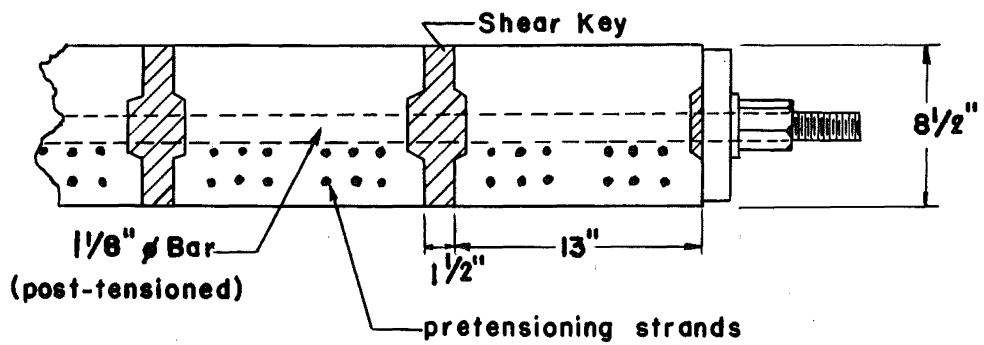## PERSPECTIVE VIEW

TYPICAL CROSS SECTION

FIG. 1 — THE TEST BRIDGE

B. THE BASIS OF LATERAL LOAD DISTRIBUTION

1. The Assumed Load Carrying System of Multi-Beam Bridges

An exact physical interpretation of the manner in which a multi-beam bridge transmits an externally applied load to its supports is somewhat complex because, not only may the structure be non-homogeneous and anisotropic, but also discontinuous due to slip between adjacent beams. In order to treat the problem mathematically, we must introduce simplifying assumptions, which in reality do not always hold true. The mathematical solution of the plate equation, for example, is made possible only by assuming that no slip occurs. As we shall show later this assumption may be far from valid.

The different possible load-carrying systems, with their respective assumptions, are given in tabular form on the following page. For a more extensive treatment of this subject, we refer to Progress Report No. 10 (A. Roesli, "Lateral Load Distribution in Multi-Beam Bridges," Lehigh University, July, 1955).

The analysis of a gridwork (with or without consideration of the torsion) is mathematically easy to express. However, in order to obtain reasonable accuracy, one must take into account many redundants, making this method somewhat lengthy. On the other hand, simplification of the analysis by means of finite differences produces very inaccurate results for concentrated loads.

Another possibility would be to consider the multi-beam bridge acting as a plate. The isotropic plate (i.e., a plate with the same bending properties in all directions) is only mentioned for completeness of discussion, because in practice the degree of lateral post-tensioning is never great enough to raise the lateral bending stiffness to the level of the longitudinal one. For a practical approach we must therefore assume that the bridge acts as an orthotropic plate, wherein the lateral bending stiffness EI_x is smaller than the longitudinal bending stiffness EI_y.* Finding the solution of an orthotropic plate problem involves excessive calculations. In Progress Report No. 10, A. Roesli has presented the latter solutions for the most important loading conditions and for bridges of various sizes; hence, the designer's problem of finding the internal forces is reduced to a simple interpolation of values taken from the tables of the mentioned report.

The question arises as to whether or not the simplifications necessary in the theory of orthotropic plates are of negligible influence. At this point we are not concerned with the formal assumptions of the plate theory. We are specifically interested in the effects of slip, which cannot be taken into account mathematically. As proved later in this paper, slip may occur in practice. Furthermore, even when small, slip has a decisive influence on the deflection and thus on the internal forces — especially the bending moments.

Nevertheless, the analysis of our problem based on the assumptions of an orthotropic plate remains the best existing approximation for the analysis of multi-beam bridges. As will be seen later, it is possible to modify this method according to the amount of existing slip in a very simple manner.

---

* Since the modulus of elasticity is considered constant, the expression $(EI)_x$ can be replaced by EI_x.

POSSIBLE ASSUMPTIONS OF LOAD CARRYING SYSTEMS

(A)

GRIDWORK

(1)   (2)

Torsion neglected	Torsion considered

Consists of a network of beams in which there are two systems of parallel beams spanning orthogonal directions.

(B)

ORTHOTROPIC PLATE

(1)   (2)

No slip between adjacent beams

Plate with different lateral and longitudinal bending stiffnesses.

$$\alpha = \frac{(EI)_y}{(EI)_x}$$

Slip between adjacent beams

Plate with discontinuous lateral bending and sheer stiffness.

LIMITING CASES

ISOTROPIC PLATE

Plate with uniform bending properties in all directions.

$$(EI)_x = (EI)_y$$
$$\alpha = 1$$

ARTICULATED PLATE

Plate with no lateral bending stiffness.

$$(EI)_y = 0$$
$$\alpha = 0$$

Lateral load transmission only by shear.

Notation: $(EI)_x =$ Longitudinal bending stiffness per unit width.

$(EI)_y =$ Lateral bending stiffness per unit width.

$$\alpha = \frac{(EI)_y}{(EI)_x}$$

4

2. The Distribution of Internal Forces and Deflections of Orthotropic Plates

The design of multi-beam bridges is governed principally by the longitudinal bending moments (M_x). Hence, the most important characteristic of such a structure is the lateral distribution of these moments over the cross section of the bridge. This moment distribution is generally known as the "lateral load distribution," probably to avoid confusion with the terminology used in Hardy Cross' method of stress analysis. This expression is somewhat misleading, because it is not the load which is distributed but only the internal forces and moments. The term "lateral load distribution" should be used only as a collective expression for the combined action of all the bridge members under a concentrated load. The idea of dividing the load into parts, proportional to the longitudinal bending moments of each beam, may be expedient for design purposes, but it does not give the correct picture of the true plate action. In a plate the load is not only transmitted by the longitudinal bending (M_x), but also by the lateral bending moments (M_y), the twisting moments (M_{xy} and M_{yx}), and the shear forces (Q_x and Q_y). As Fig. 2 illustrates, their distribution over a cross-section is quite different. (This example is for the particular case where: $\alpha = 0.5$, B/L = 0.5, a/h = 1.0 center loading).

Since internal forces cannot be measured directly, it is necessary to relate them theoretically with the deformations, which can be obtained directly from tests. This was done by using the theory of orthotropic plates.

Of special interest is the relationship between longitudinal bending moments and deflections. It should be noticed that these moments are not proportional to the deflections. Therefore, the distribution curves for the moment coefficients* and the deflection coefficients are not identical. This can be visualized by considering the following: with a concentrated load at the center point of the bridge, the deflected shape of an edge beam is somewhat similar to the shape of a uniformly loaded beam, whereas, the middle beam acts more or less like a simple beam under a single concentrated load. The moment-deflection ratio for these two cases differs by 25 per cent. Another explanation may be found in the theory of thin plates, where under a point load, the maximum deflection is finite; yet the maximum moment theoretically approaches infinity. In the practical case of a multi-beam bridge, these effects lead to a deviation between the coefficients of the longitudinal bending moments and the deflection coefficients which may be as high as 50 per cent.

---

*It is convenient to present distribution coefficients, rather than the actual moments, shear forces or deflections, themselves. The coefficient for a particular point is defined as the ratio of the moment (shear force or deflection) at this point to the average moment (shear force or deflection) of the entire cross-section. These coefficients are dimensionless and — in the range of elastic deformation — independent of the amount of load.
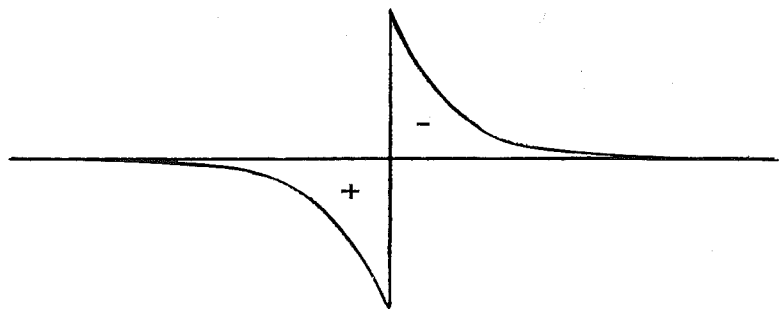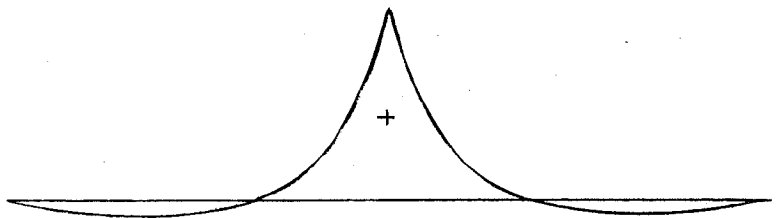
Beam Cross Section
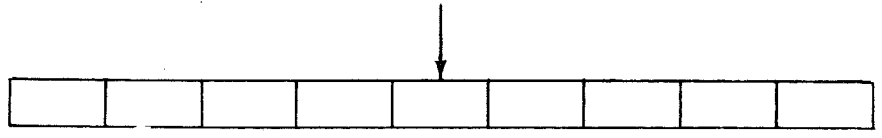
Longitudinal Bending
Moment (M$_x$)
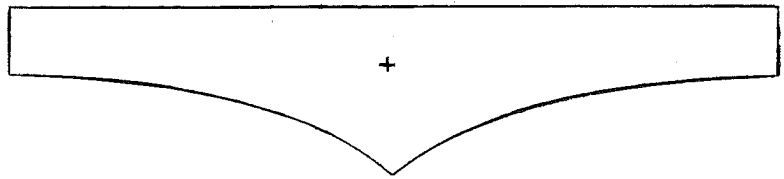
Shear Force (Q$_y$)

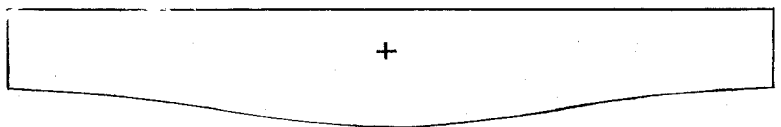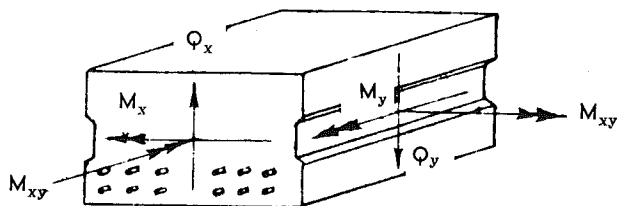Lateral Bending
Moment (M$_y$)

Deflection (w)

FIG. 2

DISTRIBUTION OF MOMENTS, SHEAR FORCES AND DEFLECTIONS

AT THE MIDSPAN CROSS-SECTION (center loading)

Magnitude of the parameters for this particular case:

B/L = 0.5;   a = 0.5;   a/h = 1.0

3. The Parameters of the Theory of Orthotropic Plates

According to the theory of orthotropic plates the internal forces or their distribution coefficients depend on three parameters:

$$\frac{B}{L} = \frac{\text{half the bridge width}}{\text{total bridge length}}$$

$$\frac{a}{h} = \frac{\text{width of one beam}}{\text{depth of one beam}}$$

$$\alpha = \frac{EI_y}{EI_x} = \frac{\text{lateral bending stiffness}}{\text{longitudinal bending stiffness}}$$

The first parameter is merely dependent on the geometry of the bridge. The second one is a function of the cross-section of the bridge members—the beams. It replaces the coefficient of torsional rigidity, which occurs in the differential equation of the orthotropic plate. The relationship of a/h and the torsional rigidity was found by theoretical considerations, which are explained in Progress Report 10.

The derivation of the parameter α is somewhat difficult and no theoretical approach has yielded satisfactory results; the reason being that the lateral bending stiffness is by no means a constant. It varies not only from point to point in the bridge, but it is also dependent on the magnitude and location of the concentrated load. This can be visualized by considering a transverse strip taken out of the bridge. It consists of rectangular blocks with no mutual cohesion; the lateral bending stiffness is provided only by the post-tensioning (Fig. 3). In practice this post-tensioning force is never large enough to prevent small openings at the bottom of the joints. In these joints, the stress distribution becomes similar to one of a cracked cross-section of a prestressed beam, i.e., this cross-section is inhomogeneous. The moment of inertia of an inhomogeneous section is variable under the combined action of moments and normal forces (post-tensioning), making it impossible to derive α theoretically. This is one of the main reasons why an empirical investigation on a laboratory bridge was necessary. It yielded simple empirical formulas for an average

α value over the entire bridge, as a function of the load and the total post-tensioning only.

If slip occurs between adjacent beams, the problem of what should be called the lateral bending stiffness becomes more complex. Due to this discontinuity (slip), the deflections and the stress distribution do not follow the rules of the plate theory at all. The idea of compensating for the effect of slip by reducing the lateral bending stiffness would lead to a contradiction, because in the case of an articulated plate, where a development of slip is very likely, the lateral bending stiffness is zero and cannot be reduced. Therefore, it was arbitrarily assumed that slip does not change the lateral bending stiffness, or in other words, that α is independent of slip. The effect of slip was taken into account by increasing the longitudinal bending moments as follows: the ratio of moment coefficient to deflection coefficient in the case with no slip was calculated for each point of the cross-section. The actual moment coefficients (considering slip) were obtained by multiplying the coefficients of the measured deflections by this ratio. This procedure, although far from being theoretically correct, was felt to be justified, since it overestimates the maximum bending moment which can occur under such conditions.
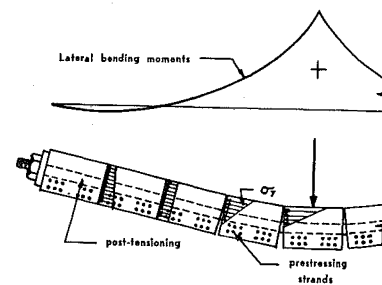

FIG. 3
DISTRIBUTION OF CONCRETE - STRESSES, ALONG A BRIDGE CROSS SECTION.

It illustrates the effects of the lateral bending moments on the stress distribution. As the lateral moment increases, the joint between adjacent beams opens, causing a reduction in the lateral moment of inertia, I_y. Thus $\alpha = EI_y/EI_x$ varies over the entire beam.

7

C. THE TESTS

1. GENERAL

In order to carry out the objectives (Part I, Introduction), the dimensions of the laboratory bridge were chosen large enough to give a reliable comparison with an actual bridge, but were limited to some extent by the available facilities. The bridge of nine beams, with which the majority of tests were performed, had a span of 16 ft. and a width of 10 ft. 9 in. (Fig. 1). Prestressing was applied in two directions, namely: longitudinally by means of pretensioning the twelve 5/16 in. strands in each beam, and laterally by post-tensioning with five 1⅛ in. Stressteel bars, located at the center, the quarter points and over the supports of the bridge. This system was convenient because the lateral post-tensioning could easily be varied, during the course of the tests, to any desired degree. The cross-sectional properties of the individual beams forming the bridge are given in Fig. 4.

To study the transfer of the shear forces, large keyways were put along the sides of the beams; in the first test series (see Program) the keyways were filled with wood so that only friction participated in this transfer, whereas real shear transfer was realized in the second series by means of grouted concrete shear keys. Because of the initial warping of the beams, additional concrete had to be placed between adjacent beams (spaced 1½ in.) to guarantee a full bearing area for the lateral post-tensioning.

All tests were performed on the newly completed test bed of the Fritz Engineering Laboratory (Fig. 5). The loads were applied by the Amsler Equipment (hydraulic jacks fed by a pendulum manometer. A detailed description of this test equipment can be found in a paper by B. Thürlimann and W. J. Eney.*

---

* B. Thurlimann and W. J. Eney
Modern Installation for Testing of Large Assemblies Under Static and Fatigue Loading. Fritz Laboratory Report No. 237-7. Lehigh University.
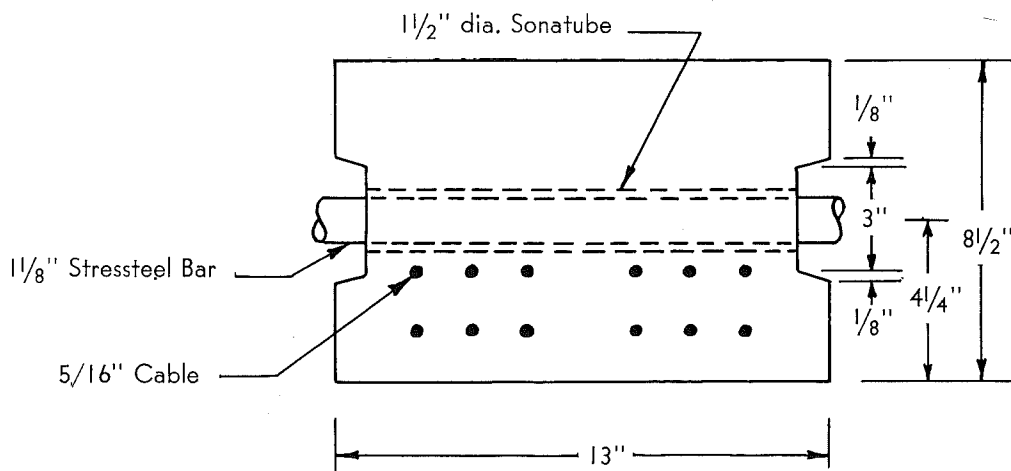

FIG. 4
BEAM CROSS SECTION

Cross Section
Width (a) — 13 in.
Depth (h) — 8½ in.   a/h = 1.53
Pretensioning (after 20% loss)
Strands - 12 — 5/16 in. cables
Tensioning Force/Strand— 7,700 lbs.
Total Tensioning Force — 92,400 lbs.
Moment of Inertia — 664 in4
Concrete Cylinder Strength — 4,540 psi

FIG. 5
TEST SET-UP OF THE LABORATORY BRIDGE

FIG. 6
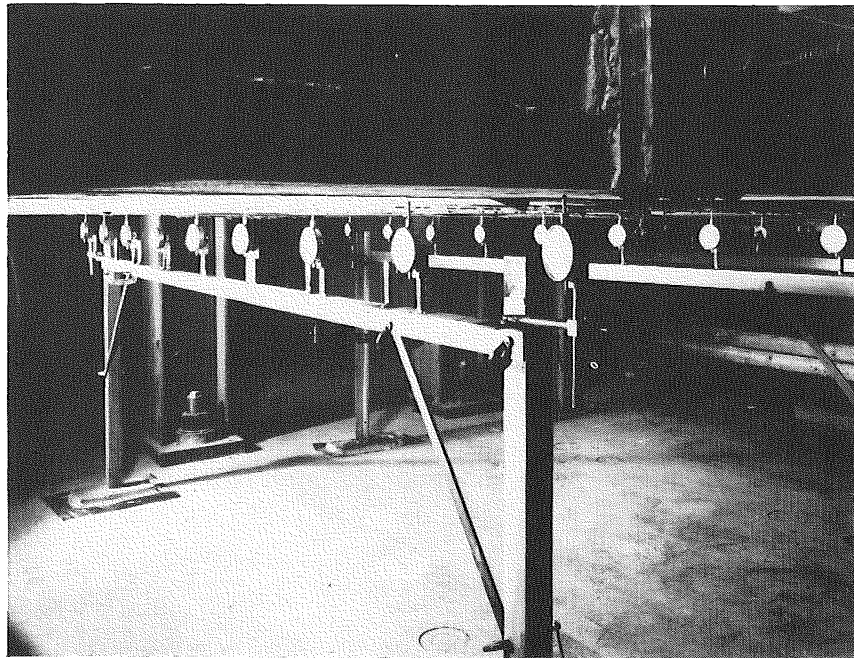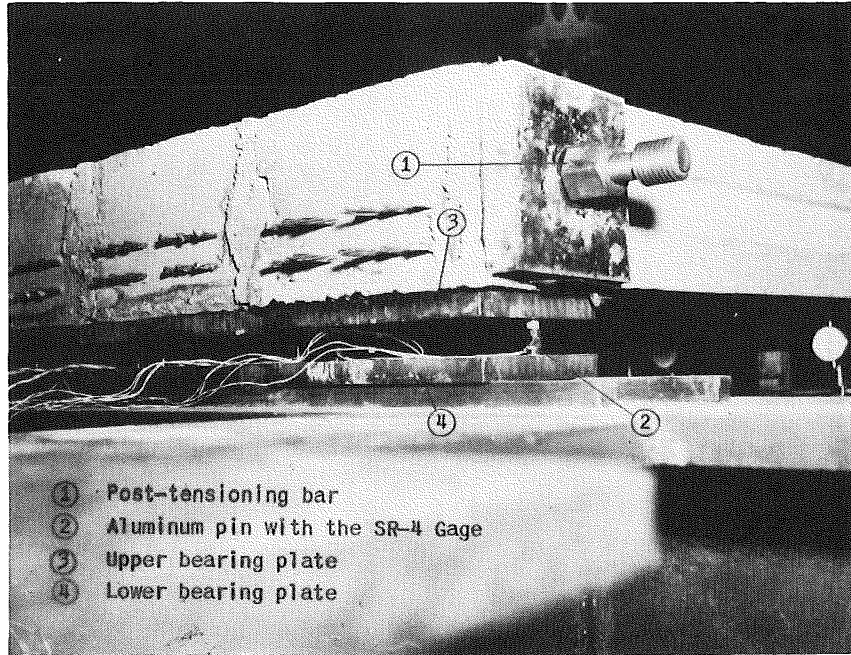DEFLECTION GAGES ON FRAMES

① Post-tensioning bar
② Aluminum pin with the SR-4 Gage
③ Upper bearing plate
④ Lower bearing plate

FIG. 7
REACTION DYNAMOMETER

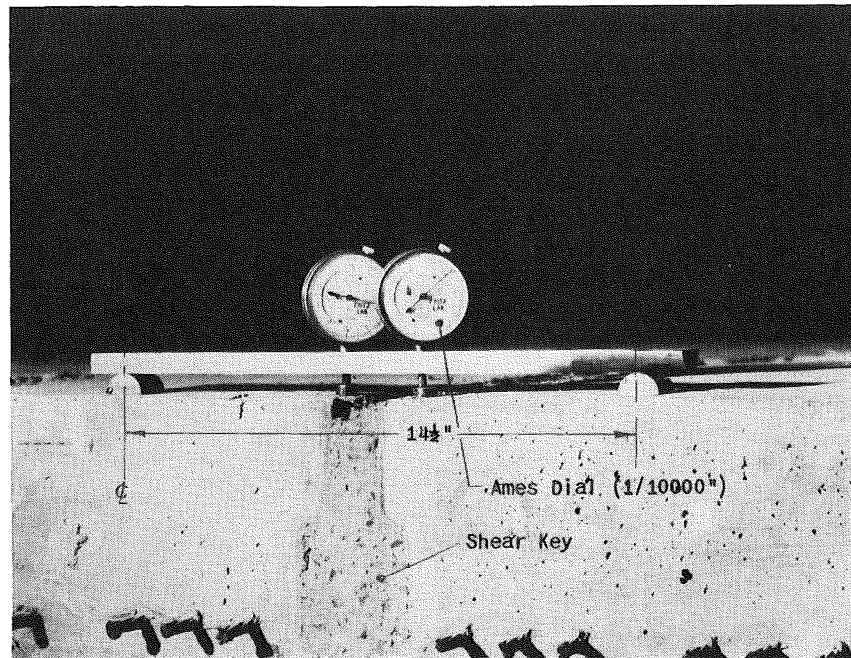
14½"
Ames Dial (1/10000")
Shear Key

FIG. 8
EQUIPMENT TO MEASURE SLIP BETWEEN
ADJACENT BEAMS

10

2. THE INSTRUMENTATION

a. Deflection

The most conclusive data in a plate investigation — as was our laboratory bridge test — are the deflections; if the deflected shape of the bridge is known in all details, all internal forces, reactions etc., can be found by differentiation. Therefore, the comparison between the theoretical and the actual behavior of the bridge was essentially a comparison between the theoretical and actual deflections.

The deflections were measured at the centerpoint and at the quarterpoints of each bridge member by means of Ames Dial Gages (sensitivity 1/1000 in.). Fig. 6 shows some of the 29 gages mounted on measuring frames. For the final destruction test, the dial gages were replaced by scales, in order to permit measurements up to the ultimate load.

b. Reactions

The reactions at the support of each beam were measured with reaction-dynamometers, each consisting of two aluminum pins and two bearing plates (Fig. 7). The shortening of the pins was measured by electrical strain gages (SR4) glued diametrically opposite on the pins. The upper bearing plate was grouted to each beam; the lower bearing plates, in which the pins were fixed, were supported either by rollers or by rectangular bars, depending on whether the dynamometer was placed at the fixed or movable end of the bridge.

c. Slip

Answering the important question, "Does slip occur and if so, how much?" required a precise measuring device; because, even when very small, the slip has a decisive effect on the distribution of deflections and internal forces. This high precision was achieved by measuring directly the relative slip between two adjacent beams (Fig. 8): two dial gages (sensitivity 1/10,000 in.) were fixed on a rectangular bar which spanned the two beams from center to center. Small half-round bars, fixed with sealing wax

to the beams, served as a support for the device. The points of the dials touched two small bearing plates on both sides of the shear keys.

3. THE TEST PROGRAM

The 58 different tests, performed in a sequence dictated by the operations they involved, can be divided into three major categories, which are:

(1) Tests to determine the stiffness properties of the bridge
    a. The properties of the individual beams
    b. The longitudinal bending stiffness of the bridge
    c. The lateral bending stiffness of the bridge
    d. The torsional rigidity of the bridge

(2) Tests to investigate the influence of
    a. Degree of lateral post-tensioning
    b. Location of lateral post-tensioning
    c. Location of the external load
    d. Interaction of shear keys
    e. Slip between adjacent beams

(3) Tests to determine the lateral load distribution in the inelastic range up to destruction of the bridge.

Table I gives a description, the numeration and some important results of the tests.

First, an individual beam was tested to destruction, in order to find the elastic and plastic deflections, the cracking load and the ultimate load of the bridge members (Fig. 9).

The tests (70 to 82) to determine the elastic properties of the entire bridge (EI_x, EI_y, etc.) were all performed with grouted shear keys, varying only the post-tensioning force of the bars. Fig. 10 shows the setup of tests 80, 81 and 82.

The bridge was supported across the ends, the jack load being distributed to a line load by a heavy I-beam. These tests yielded values for the longitudinal bending stiffness, EI_x.

The lateral bending stiffness was found similarly (tests 70 to 72, Fig. 11): with lon-
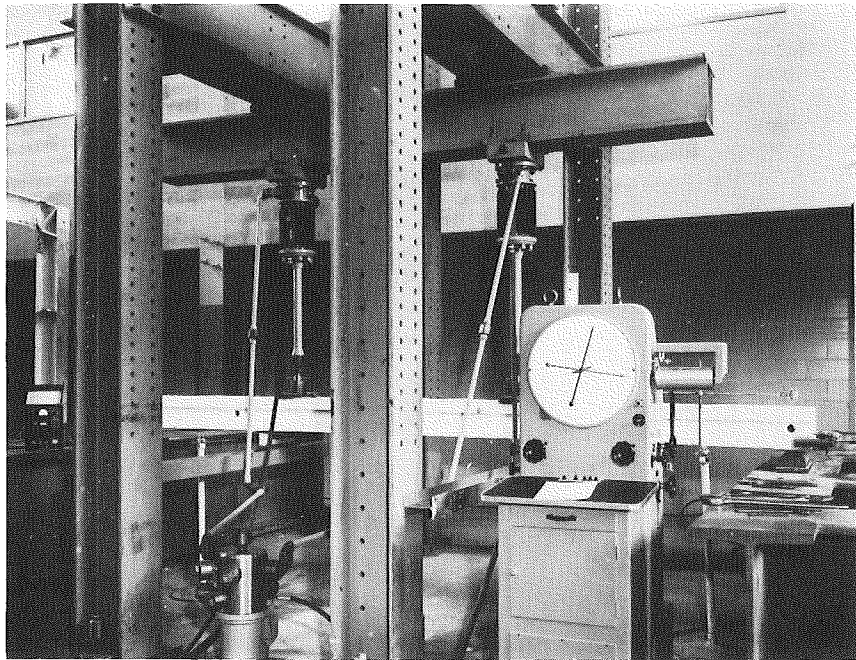
TESTS PERFORMED AND RESULTS
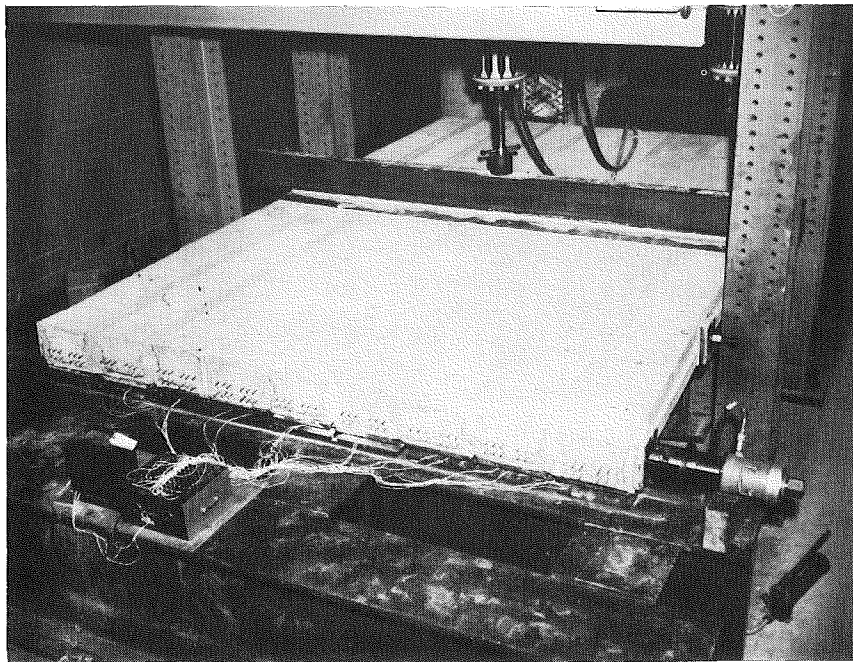
FIG. 9
DESTRUCTION TEST OF AN INDIVIDUAL BEAM

FIG. 10
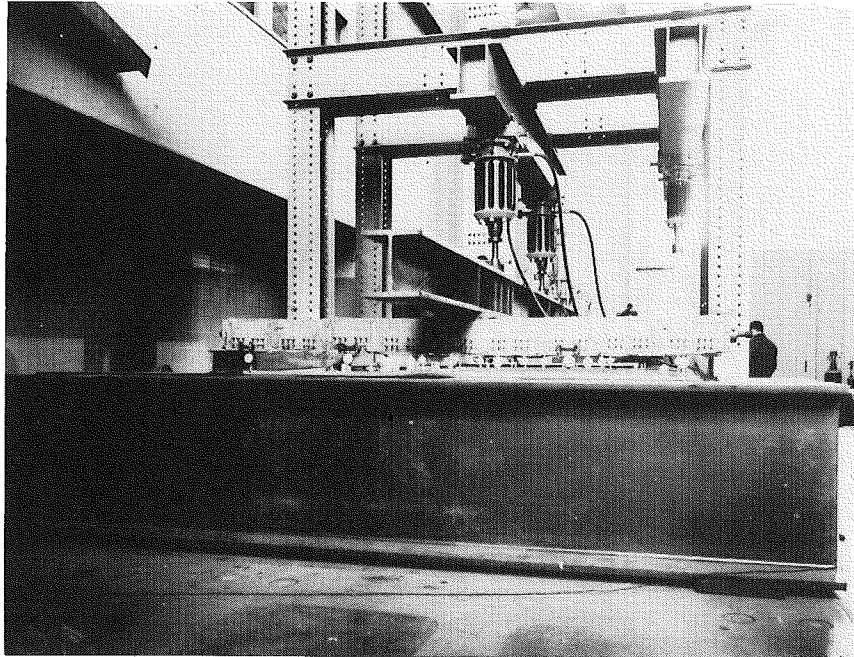DETERMINATION OF THE LONGITUDINAL
BENDING STIFFNESS

FIG. 11
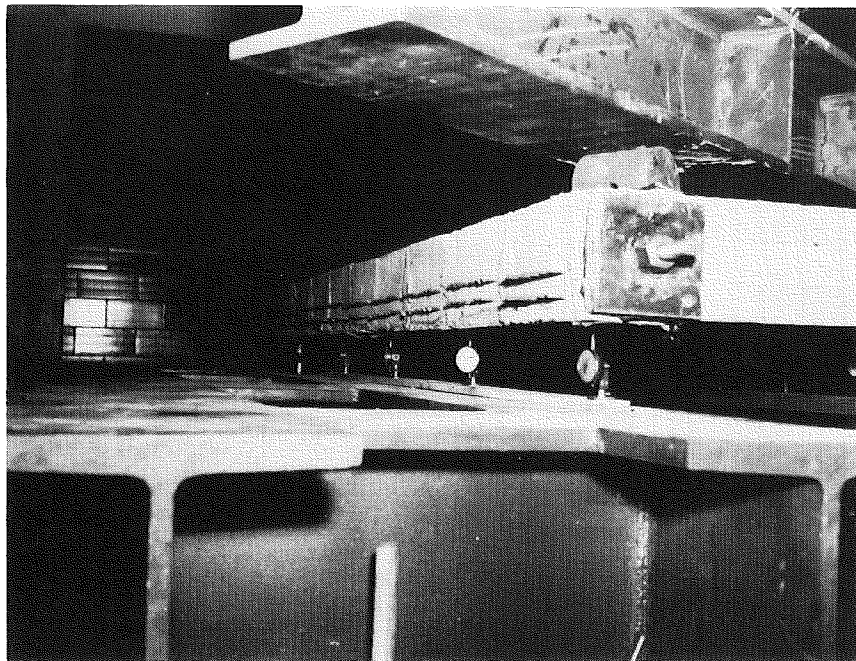DETERMINATION OF THE LATERAL
BENDING STIFFNESS

FIG. 12
DETERMINATION OF THE TORSIONAL RIGIDITY

gitudinal supports along the two edge beams and a line load along the center beam.

During the tests for the determination of the torsional rigidity (tests 75 to 77, Fig. 12) the bridge was in an indifferent state of equilibrium: two diagonally related corners were loaded, the other two supported. The load was transmitted to the corners by an I-beam, supported by half round blocks at the other two corners; the reactions were taken by spherical bearings. Since these tests implied a certain risk of local destruction, they were performed after the important tests 3 to 65.

The investigation of different influencing factors (tests 3 to 65) represents the essence of this study. The variation of these factors could not follow a logical sequence as given in the beginning of this chapter. Since many operations such as changing jacks, grouting of the shear keys, etc., were involved, the sequence of tests was dictated by practical considerations.

The variation of the shear-transfer leads to two major groups: Tests without shear keys (with or without grouting) and tests with shear keys (Fig. 13).

With the exception of tests 2 to 6 (determination of the influence of the ratio B/L) the two groups involved the same variables, namely: the degree and location of lateral post-tensioning and the location of the concentrated load. Only the two load conditions, which can yield maximum moments, were considered, i.e., a load at the center point of the bridge and a load at midspan of the edge beam. The post-tensioning was varied by choosing different forces in the bars as well as by changing the number of bars. The variation of the slip measurements in these tests was big enough, so that no separate tests for the determination of its influence were necessary.

Finally the lateral load distribution was studied in the inelastic range of deflection. This test (No. 90), up to destruction, was performed with five kips post-tensioning on each of the five bars and with a concentrated load at midspan.

The extensive testing necessary in this investigation covered a period of three months.

WITHOUT SHEAR KEY, JOINTS GROUTED
(Keyway filled with wood)

wood — grouting
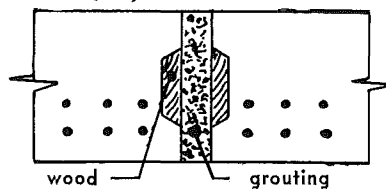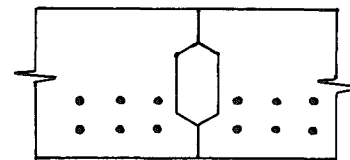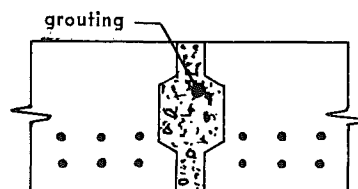
WITHOUT SHEAR KEY
JOINTS NOT GROUTED

FIG. 13

WITH GROUTED SHEAR KEY
grouting —

15

D. THE TEST RESULTS

Rather than to present all the test results, involving about 30,000 readings, an effort will be made in this chapter to show the relationship between the different influencing factors. The most important data, however, is given in the Tables 1, 2a-f.

1. THE STIFFNESS PROPERTIES OF THE BRIDGE

a. The properties of the individual beams

Preliminary to the bridge tests, a single beam was tested under third-point loading up to failure (Fig. 9). The load-deflection (respectively moment-deflection) curve is shown in Fig. 14.

The bending stiffness before cracking was 25×10^8 lb. in.^{2}. In order to compare this value with the bending stiffness of the bridge —in plate problems always given per unit width—it had to be divided by the width of the beam (13 in.); i.e.,

$$EI_x = 196 \times 10^6 \text{ lb. in.}^2/\text{in.}$$

b. The longitudinal and lateral bending stiffness of the bridge

Due to the effect of the lateral contraction (Poisson's Ratio) and the fact that the joints of the beams were grouted, the longitudinal bending stiffness per unit width of an individual beam and of the entire bridge was different, furthermore the latter depends on whether or not one includes the grouting in the total bridge width.

Longitudinal Bending Stiffness
(per unit width)
Single Beam $EI_x = 196 \times 10^6$ lb.in.^{2}/in.
Entire Bridge
 grouting excluded $EI_x = 205 \times 10^6$ lb.in.^{2}/in.
 grouting included $EI_x = 185 \times 10^6$ lb.in.^{2}/in.

From the first two values we can conclude that the effect of Poisson's Ratio increased the bending stiffness about 5 per cent. In both cases, single beam and bridge, the longitudinal bending stiffness could be
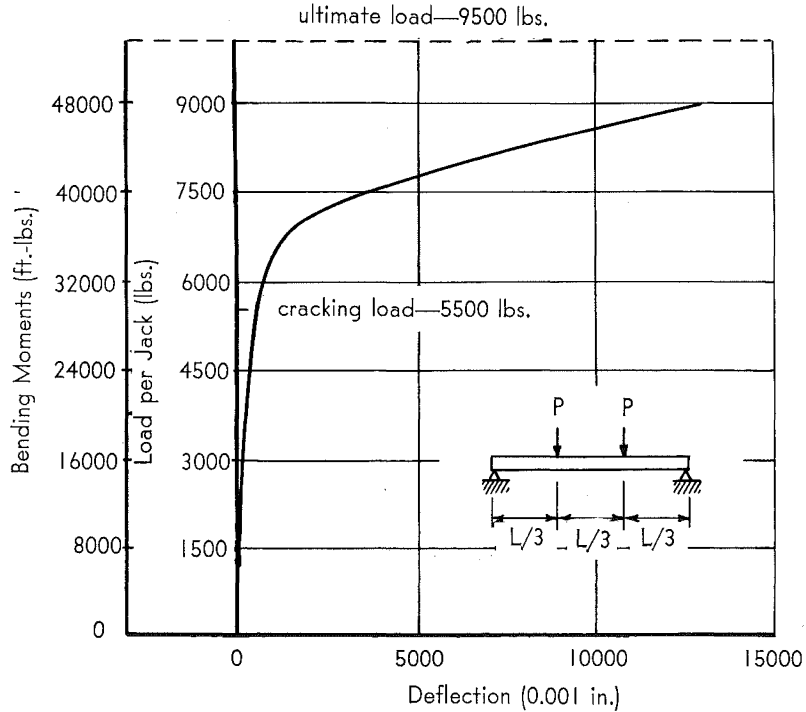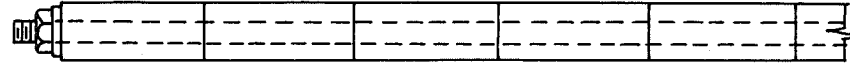

ultimate load—9500 lbs.

cracking load—5500 lbs.

Bending Moments (ft.-lbs.)

Load per Jack (lbs.)

Deflection (0.001 in.)

FIG. 14
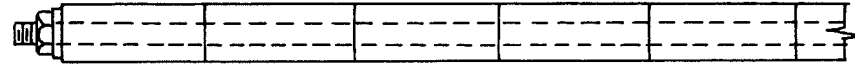**LOAD (MOMENT) — DEFLECTION CURVE**
OF AN INDIVIDUAL BEAM

Test No.	Figure	Post-tensioning (tons/bar)	Load (Kips)	Conditions	Partial Cross Section DEFLECTIONS AND COEFFICIENTS*					Alpha	Slip 1/1000"
3		30	10	Without			105 (1.00)	105 (1.00)	107 (1.02)		
			20	shear key;			227 (0.99)	227 (0.99)	233 (1.02)	0.73	
			27.5	5 beams			327 (0.99)	330 (1.00)	336 (1.02)		
4		10	10	Without			110 (0.99)	111 (1.00)	115 (1.04)		
			20	shear key;			224 (0.99)	228 (1.00)	237 (1.04)	0.44	
			27.5	5 beams			315 (0.97)	325 (1.00)	339 (1.05)		
5		30	10	Without		84 (0.98)	86 (1.00)	86 (1.01)	90 (1.05)		
			20	shear key;		173 (0.97)	178 (0.99)	182 (1.01)	188 (1.05)	0.73	
			30	7 beams		263 (0.95)	271 (0.99)	283 (1.03)	293 (1.07)		
6		30	10	Without		83 (0.95)	86 (0.99)	90 (1.03)	93 (1.07)		
			20	shear key;		166 (0.93)	175 (0.98)	187 (1.05)	196 (1.09)	0.39	
			30	7 beams		244 (0.91)	264 (0.97)	290 (1.07)	302 (1.11)		
10		30	10	Without	63 (0.89)	68 (0.94)	75 (1.03)	80 (1.07)	84 (1.16)		7
			20	shear key;	126 (0.86)	135 (0.93)	150 (1.03)	165 (1.11)	176 (1.19)	0.65	37
			30	9 beams	177 (0.86)	200 (0.92)	225 (1.02)	252 (1.12)	270 (1.23)		74
11		20	10	Without	59 (0.80)	68 (0.92)	77 (1.04)	85 (1.15)	90 (1.22)		9
			20	shear key;	116 (0.79)	134 (0.90)	152 (1.03)	172 (1.16)	185 (1.25)	0.58	52
			30	9 beams	170 (0.77)	196 (0.90)	226 (1.03)	259 (1.18)	281 (1.28)		76
12		10	10	Without	53 (0.76)	63 (0.88)	73 (1.03)	85 (1.20)	93 (1.31)		17
			20	shear key;	109 (0.76)	127 (0.88)	147 (1.02)	172 (1.19)	191 (1.32)	0.50	64
			30	9 beams	161 (0.75)	189 (0.88)	219 (1.02)	266 (1.19)	286 (1.33)		114
13		5	10	Without	53 (0.75)	62 (0.87)	73 (1.03)	86 (1.21)	94 (1.32)		35
			20	shear key;	106 (0.74)	124 (0.87)	145 (1.02)	171 (1.20)	193 (1.35)	0.38	95
			30	9 beams	158 (0.74)	185 (0.87)	217 (1.01)	258 (1.21)	293 (1.37)		166
14		2.5	10	Without	51 (0.74)	60 (0.87)	70 (1.01)	84 (1.22)	92 (1.33)		30
			20	shear key;	104 (0.73)	121 (0.86)	142 (1.01)	171 (1.21)	197 (1.39)	0.27	142
			30	9 beams	154 (0.73)	181 (0.85)	215 (1.01)	257 (1.21)	302 (1.42)		277

NOTATIONS:

● Point of load

* Figures without parenthesis are measured deflections in thousandths of an inch.
  Figures in parenthesis are the coefficients of deflection.
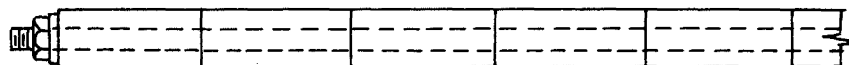
TABLE 2a

17

Partial Cross Section

No.	Figure	Post-tensioning (tons/bar)	Load (Kips)	Conditions	DEFLECTIONS AND COEFFICIENTS*					Alpha	Slip 1/1000"
15		1	10	No	51 (0.74)	60 (0.87)	71 (1.02)	84 (1.21)	91 (1.32)		33
			20	shear	103 (0.72)	121 (0.85)	144 (1.01)	173 (1.21)	203 (1.42)	0.20	112
			30	key	153 (0.71)	182 (0.84)	218 (1.00)	262 (1.21)	324 (1.49)		199
20		30	10	No	51 (0.79)	59 (0.90)	68 (1.05)	75 (1.16)	76 (1.18)		1
			20	shear	96 (0.70)	119 (0.87)	144 (1.05)	167 (1.22)	185 (1.34)	0.34	43
			30	key	139 (0.66)	177 (0.84)	220 (1.04)	262 (1.26)	302 (1.43)		83
21		20	10	No	47 (0.68)	59 (0.86)	72 (1.04)	83 (1.21)	97 (1.41)		17
			20	shear	88 (0.61)	118 (0.82)	150 (1.04)	186 (1.29)	217 (1.50)	0.22	59
			30	key	128 (0.59)	177 (0.82)	226 (1.04)	277 (1.28)	337 (1.56)		103
22		10	10	No	42 (0.60)	56 (0.80)	73 (1.05)	92 (1.31)	105 (1.38)		13
			20	shear	80 (0.56)	113 (0.78)	152 (1.05)	191 (1.32)	230 (1.50)	0.10	53
			30	key	118 (0.54)	167 (0.77)	227 (1.05)	287 (1.32)	355 (1.59)		87
23		5	10	No	40 (0.55)	54 (0.75)	75 (1.05)	95 (1.33)	116 (1.63)		19
			20	shear	76 (0.52)	109 (0.75)	152 (1.04)	197 (1.35)	250 (1.71)	0.095	87
			30	key	113 (0.52)	162 (0.74)	226 (1.03)	293 (1.34)	389 (1.77)		254
25		30	10	No	58 (0.84)	63 (0.91)	70 (1.01)	77 (1.12)	85 (1.23)		12
			20	shear	113 (0.80)	128 (0.91)	145 (1.03)	160 (1.13)	182 (1.29)	0.50	48
			30	key	165 (0.76)	191 (0.88)	221 (1.02)	261 (1.20)	284 (1.31)		91
26		20	10	No	55 (0.81)	62 (0.92)	69 (1.01)	78 (1.16)	84 (1.24)		10
			20	shear	107 (0.75)	128 (0.90)	144 (1.01)	167 (1.18)	189 (1.33)	0.34	40
			30	key	158 (0.71)	190 (0.86)	226 (1.03)	266 (1.21)	314 (1.42)		97
27		15	10	No	54 (0.75)	63 (0.89)	73 (1.02)	84 (1.19)	93 (1.31)		11
			20	shear	105 (0.72)	126 (0.86)	151 (1.03)	176 (1.20)	209 (1.42)	0.34	25
			30	key	155 (0.70)	187 (0.86)	227 (1.03)	269 (1.22)	317 (1.43)		57
28		10	5	No shear	27 (0.83)	29 (0.91)	34 (1.03)	38 (1.17)	37 (1.14)	0.34	19
			30	key	149 (0.69)	181 (0.84)	229 (1.06)	262 (1.21)	308 (1.42)		106

NOTATIONS:
● Point of load
* Figures without parenthesis are measured deflections in thousandths of an inch.
Figures in parenthesis are the coefficients of deflection.
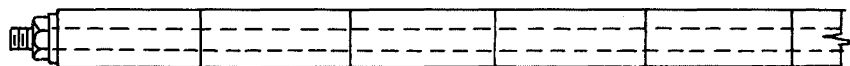
TABLE 2b

18

Test No.	Figure	Post-tensioning (tons/bar)	Load (Kips)	Conditions	Partial Cross Section DEFLECTIONS AND COEFFICIENTS*					Alpha	Slip 1/1000"
29		5	5	No shear	27 (0.79)	30 (0.88)	36 (1.07)	39 (1.16)	41 (1.22)		37
			30	key	141 (0.66)	178 (0.83)	222 (1.03)	265 (1.24)	318 (1.44)	0.20	135
32		15	5	No shear	26 (0.75)	29 (0.85)	34 (1.00)	40 (1.16)	52 (1.52)		32
			26	key	130 (0.66)	154 (0.79)	187 (0.96)	224 (1.14)	377 (1.92)	0.09	335
33		10	5	No shear	25 (0.72)	29 (0.83)	34 (0.99)	40 (1.17)	55 (1.60)		38
			24	key	119 (0.66)	141 (0.78)	171 (0.95)	206 (1.14)	354 (1.96)	0.09	81
34		5	5	No shear	25 (0.72)	29 (0.83)	34 (0.99)	41 (1.18)	55 (1.60)		14
			21	key	102 (0.64)	122 (0.77)	150 (0.94)	182 (1.15)	318 (2.00)	0.09	82
45		5	5	No shear key	20 (0.58)	23 (0.69)	29 (0.86)	49 (1.47)	61 (1.83)		1825
			10	or grouting	25 (0.42)	32 (0.54)	41 (0.69)	85 (1.43)	166 (2.82)		4450
46		5	2.5	No shear key	10 (0.59)	12 (0.68)	15 (0.86)	26 (1.51)	29 (1.72)		910
			5	or grouting	20 (0.57)	21 (0.62)	28 (0.80)	54 (1.56)	59 (1.72)		885
47		5	2.5	No shear key	1 (0.06)	2 (0.12)	3 (0.18)	26 (1.49)	91 (5.32)		750
			5	or grouting	2 (0.06)	4 (0.10)	5 (0.15)	55 (1.60)	175 (5.16)		1453
48		5	2.5	No shear key	6 (0.36)	8 (0.48)	11 (0.66)	32 (1.90)	36 (2.18)		630
			5	or grouting	10 (0.30)	13 (0.37)	18 (0.53)	64 (1.89)	97 (2.86)		1438
50		30	10	With	60 (0.98)	61 (1.00)	61 (1.00)	61 (1.01)	61 (1.01)		0
			20	shear	124 (0.98)	125 (0.99)	127 (1.00)	129 (1.02)	130 (1.03)	0.65	0
			30	key	191 (0.98)	192 (0.99)	198 (1.01)	198 (1.02)	201 (1.03)		0
51		10	10	With	61 (1.00)	61 (0.98)	62 (1.00)	62 (1.00)	62 (1.01)		0
			20	shear	120 (0.97)	122 (0.98)	125 (1.01)	127 (1.02)	129 (1.04)	0.5	0
			30	key	182 (0.96)	184 (0.96)	193 (1.01)	196 (1.03)	201 (1.06)		0

NOTATIONS:

● Point of load

* Figures without parenthesis are measured deflections in thousandths of an inch.
Figures in parenthesis are the coefficients of deflection.
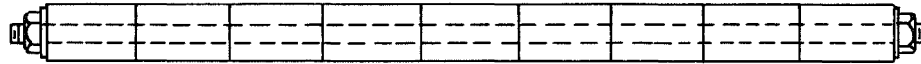
TABLE 2c

Test No.	Figure	Post-tensioning (tons/bar)	Load (Kips)	Conditions	Partial Cross Section DEFLECTIONS AND COEFFICIENTS*					Alpha	Slip 1/1000"
52		5	10 20 30	With shear key	60 (0.97) 119 (0.96) 178 (0.94)	61 (0.99) 121 (0.98) 183 (0.97)	63 (1.02) 125 (1.01) 193 (1.02)	62 (1.01) 127 (1.03) 197 (1.04)	62 (1.01) 130 (1.05) 203 (1.07)	0.38	0 0 0
53		1	10 20 30	With shear key	61 (0.98) 117 (0.92) 174 (0.92)	60 (0.97) 121 (0.96) 182 (0.96)	63 (1.01) 128 (1.01) 192 (1.02)	64 (1.02) 131 (1.03) 200 (1.06)	65 (1.05) 133 (1.05) 207 (1.09)	0.20	0 0 0
54		0	10 20 30	With shear key	56 (0.90) 113 (0.90) 169 (0.90)	59 (0.96) 119 (0.95) 178 (0.95)	62 (1.01) 127 (1.01) 190 (1.01)	66 (1.07) 136 (1.08) 204 (1.08)	68 (1.11) 141 (1.13) 214 (1.14)	0.08	0 0 0
55		30	30		176 (0.94)	180 (0.97)	187 (1.01)	195 (1.05)	200 (1.07)	0.34	0
56		10	30		172 (0.92)	179 (0.96)	188 (1.00)	200 (1.07)	207 (1.11)	0.10	0
57		5	30		170 (0.91)	178 (0.95)	188 (1.01)	201 (1.07)	210 (1.12)	0.095	0
58		1	30		169 (0.90)	177 (0.95)	188 (1.01)	202 (1.08)	211 (1.13)	0.42	0
59		0	30		171 (0.91)	178 (0.95)	188 (1.01)	201 (1.07)	210 (1.12)	0.09	0

NOTATIONS:

● Point of load

* Figures without parenthesis are measured deflections in thousandths of an inch.

Figures in parenthesis are the coefficients of deflection.
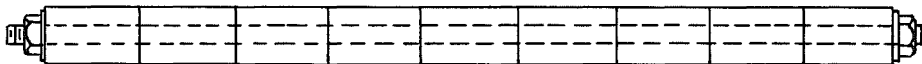
TABLE 2d

20

Test No.	Figure	Post-tensioning (tons/bar)	Load (Kips)	Conditions	DEFLECTIONS AND COEFFICIENTS*									Alpha	Slip 1/1000"
40		30	5	Without shear key	13 (0.39)	17 (0.51)	20 (0.60)	24 (0.71)	29 (0.80)	37 (1.10)	43 (1.28)	59 (1.76)	60 (1.78)		13
			10		25 (0.37)	33 (0.49)	40 (0.60)	49 (0.73)	60 (0.90)	75 (1.12)	88 (1.31)	107 (1.60)	125 (1.87)	0.28	5
			30		47 (0.34)	65 (0.48)	80 (0.59)	100 (0.73)	122 (0.89)	152 (1.11)	180 (1.32)	223 (1.63)	261 (1.91)		21
41		10	5	Without shear key	12 (0.36)	16 (0.48)	19 (0.57)	25 (0.75)	29 (0.87)	37 (1.11)	44 (1.32)	55 (1.65)	64 (1.92)		3
			10		24 (0.35)	33 (0.49)	39 (0.57)	48 (0.71)	59 (0.87)	74 (1.09)	90 (1.32)	112 (1.65)	133 (1.96)	0.27	12
			20		46 (0.34)	63 (0.46)	77 (0.56)	105 (0.77)	118 (0.86)	149 (1.09)	180 (1.31)	227 (1.66)	270 (1.97)		35
42		5	5	Without shear key	13 (0.39)	17 (0.51)	19 (0.57)	24 (0.72)	27 (0.81)	36 (1.08)	44 (1.32)	54 (1.62)	65 (1.95)		6
			10		25 (0.37)	32 (0.47)	38 (0.56)	47 (0.69)	57 (0.84)	74 (1.09)	90 (1.32)	114 (1.68)	135 (1.99)	0.26	15
			20		47 (0.34)	62 (0.45)	75 (0.54)	102 (0.74)	116 (0.84)	154 (1.11)	181 (1.31)	232 (1.67)	278 (2.01)		43
43		1	5	Without shear key	12 (0.36)	13 (0.39)	17 (0.51)	21 (0.63)	26 (0.79)	35 (1.06)	45 (1.36)	58 (1.75)	71 (2.15)		6
			10		23 (0.34)	28 (0.41)	35 (0.52)	43 (0.63)	54 (0.80)	72 (1.06)	91 (1.34)	119 (1.75)	146 (2.15)	0.19	29
			17.5		29 (0.22)	37 (0.28)	49 (0.38)	62 (0.48)	83 (0.64)	113 (0.86)	146 (1.12)	202 (1.55)	457 (3.50)		
60		30	5	Without shear key	17 (0.56)	19 (0.62)	22 (0.72)	25 (0.82)	28 (0.92)	32 (1.05)	38 (1.24)	44 (1.44)	50 (1.63)		3
			10		35 (0.56)	40 (0.64)	45 (0.72)	51 (0.82)	57 (0.91)	66 (1.06)	77 (1.23)	89 (1.43)	102 (1.63)	0.28	5
			20		71 (0.55)	81 (0.63)	91 (0.71)	105 (0.82)	119 (0.93)	137 (1.07)	158 (1.23)	183 (1.43)	209 (1.63)		7

NOTATIONS:

● Point of load

* Figures without parenthesis are measured deflections in thousandths of an inch.
Figures in parenthesis are the coefficients of deflection.

TABLE 2e

Test No.	Figure	Post-tensioning (tons/bar)	Load (Kips)	Conditions	DEFLECTIONS AND COEFFICIENTS*									Alpha	Slip 1/1000"
61		5	10	With shear key	35 (0.56)	40 (0.64)	45 (0.72)	51 (0.82)	57 (0.91)	66 (1.06)	77 (1.23)	90 (1.44)	103 (1.65)	0.26	1
			20		71 (0.56)	80 (0.63)	90 (0.71)	104 (0.82)	117 (0.92)	135 (1.06)	155 (1.22)	180 (1.42)	208 (1.64)		2
62		0	10	With shear key	35 (0.56)	39 (0.62)	44 (0.70)	51 (0.81)	57 (0.91)	67 (1.07)	78 (1.24)	91 (1.45)	104 (1.65)	0.10	0
			20		75 (0.59)	80 (0.63)	88 (0.70)	99 (0.78)	110 (0.87)	130 (1.03)	156 (1.23)	185 (1.46)	217 (1.71)		1
63		5	20	With shear key	71 (0.57)	79 (0.64)	87 (0.70)	99 (0.80)	111 (0.90)	130 (1.05)	152 (1.22)	179 (1.44)	209 (1.69)	0.10	1
64		30	20	With shear key	69 (0.56)	78 (0.63)	87 (0.70)	101 (0.81)	115 (0.93)	133 (1.07)	153 (1.23)	178 (1.43)	205 (1.66)	0.19	1
65		30	20	With shear key	75 (0.60)	82 (0.66)	90 (0.72)	100 (0.80)	111 (0.89)	130 (1.04)	152 (1.22)	179 (1.43)	208 (1.67)	0.19	1

NOTATIONS:
● Point of load
* Figures without parenthesis are measured deflections in thousandths of an inch.
Figures in parenthesis are the coefficients of deflection.

TABLE 2f

considered as constant up to the cracking load.

This did not hold true for the tests to derive the lateral bending stiffness (Fig. 11). The reason was, again, that the post-tensioning could not prevent openings between adjacent beams and thus the bending stiffness was dependent on the magnitude of the load. Fig. 15 shows the large variation of EI_y as the load increases.
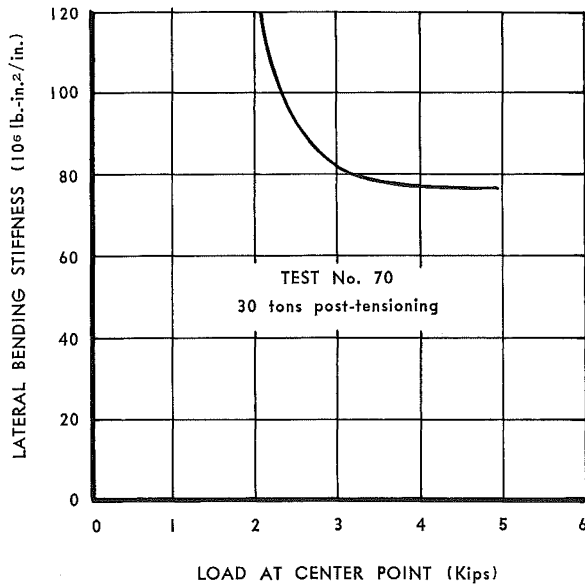

TEST No. 70
30 tons post-tensioning

LOAD AT CENTER POINT (Kips)

FIG. 15

In order to derive the factor $\propto\, = EI_y/EI_x$ from these tests, the lateral bending stiffness was taken at the point where the curve of Fig. 15 becomes horizontal, yielding the following ratios:

	POST-TENSIONING PER BAR		
	30 tons	5 tons	1 ton
$\propto$	0.41	0.0174 (obtained by line loading)	0
	0.65	0.38 (concentrated center loading)	0.20

These $\propto$ values, however, are much too small for the same bridge subjected to concentrated loads, because in this case the maximum lateral bending moments are con-

fined to a small area under the load whereas they extend over the whole length of the bridge in the prescribed tests. The experimental $\propto$ values for concentrated loads (tests 50, 52 and 53) are also given in the above table.

For this reason, the way of finding $\propto$ by separately bending the bridge longitudinally and laterally was abandoned. The method of calculating $\propto$ used in this study, will be given in section 2a of this chapter.

c. The Torsional Rigidity of the Bridge

The differential equation of an ortho-tropic plate can be written in the following form:

$$\frac{\partial^4 w}{\partial x^4} + 2\beta \frac{\partial^4 w}{\partial x^2 \partial y^2} + \propto \frac{\partial^4 w}{\partial y^4} = \frac{P(xy)}{EI_x}$$

Besides the ratio of the bending stiffness ($\propto$), it contains a coefficient 2β, called the coefficient of torsional rigidity. It can experimentally be found by loading a plate at two diagonally opposite corners and supporting the other two corners (Fig. 12). Under these loading conditions no bending moments M_x and M_y occur; the only existing internal moments acting on an element $dxdy$ are the twisting moments M_{xy} and M_{yx}.
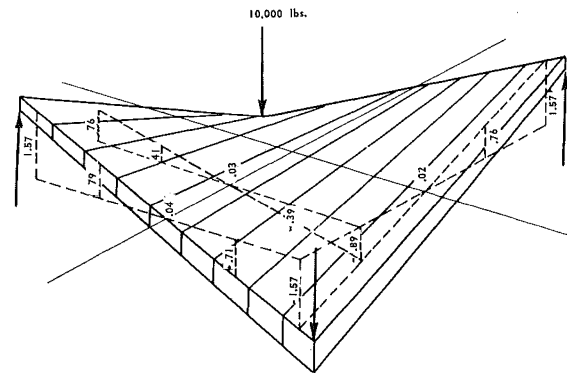

FIG. 16
TORSIONAL RIGIDITY — TEST NO. 75
(deflections in inches)

NOTE: All originally horizontal lines, which were parallel to the X axis or the Y axis, remained straight after deformation.

The deflections follow the formula:

$$w = - \frac{1}{EI_x} \frac{M_{xy} + M_{yx}}{2\beta} \, xy$$

This expression is linear in x and y, thus the deformed bridge has two straight lines as generatrices, the x and y axis. This was confirmed in the tests 75 and 76, for all beams and strips perpendicular to the beams remained approximately straight. Fig. 16 shows a perspective view of the shape of the deformed bridge, and the deflections of test 75 at the load of 10,000 lbs. at both load points.

Under these loading conditions, the twisting moments can be expressed by the load:

$$M_{xy} + M_{yx} = P$$

Hence the coefficient of torsional rigidity becomes

$$2\beta = - \frac{P}{wEI_x} xy$$

In Progress Report 10* a theoretical relationship between α and β had been established, which had to be checked by our tests.
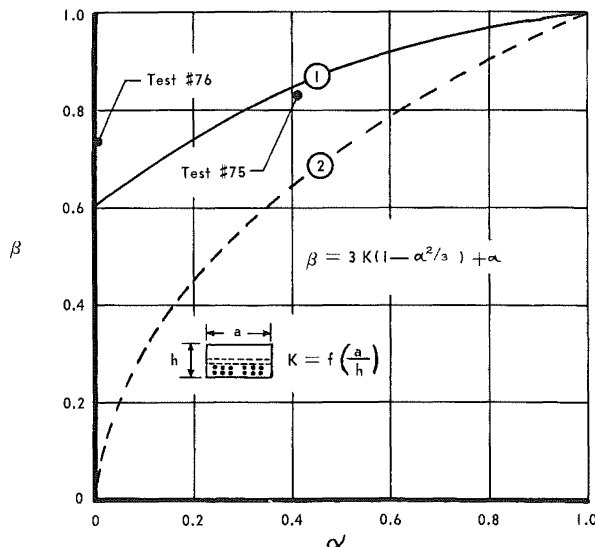

FIG. 17
RELATIONSHIP BETWEEN α AND β
(a/h = 1.5)

● Measured Relationship
(1) Theoretical curve according to A. Roesli
(2) Theoretical curve according to M. T. Huber

Fig. 17 gives the theoretical curve and the two points which resulted from tests 75 and 76.

The correlation between the empirical and theoretical results indicates that under the various assumptions proposed for this relationship, the one established by A. Roesli comes closest to reality.

Both the discussion of our test results and the résumé of the analysis are based on this theoretical relationship. Since β is a function of K and α where K depends on a/h, the effect of torsional rigidity can be expressed by the parameters α and a/h.

2. COMPARISON BETWEEN THE THEORY AND THE TESTS

a. Deflections

One of our major problems, the determination of the longitudinal bending moment of each bridge member, can be solved by using the longitudinal or the lateral deflection distribution.

The first method would make use of the formula

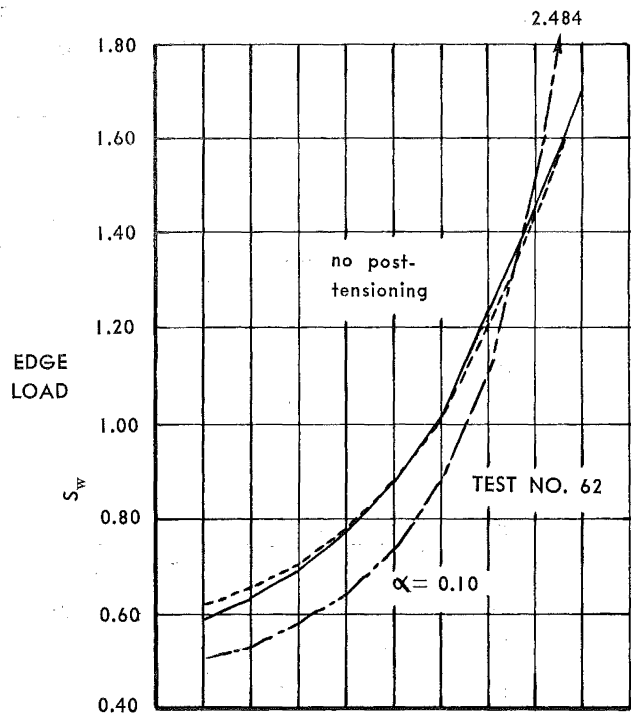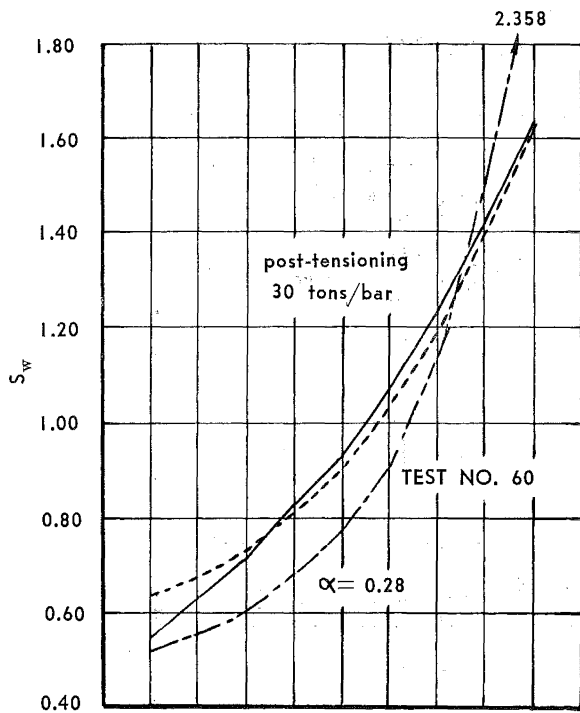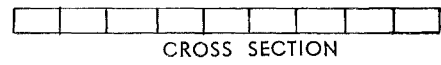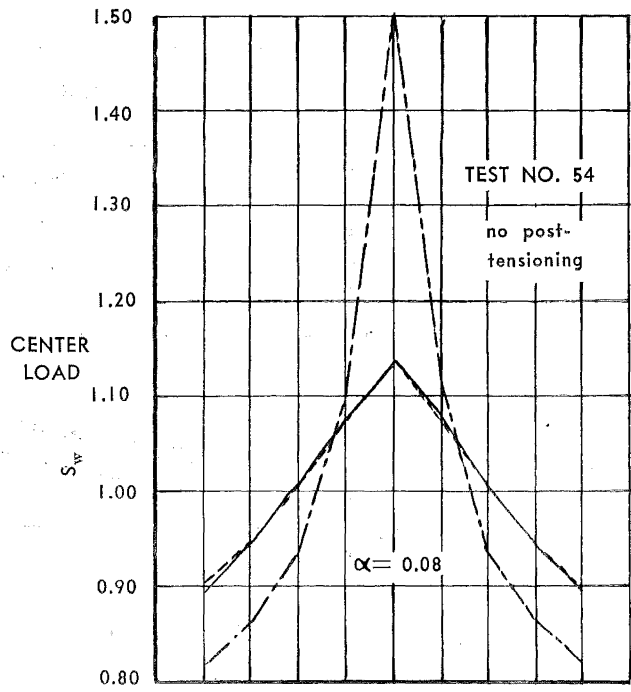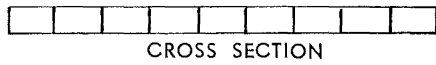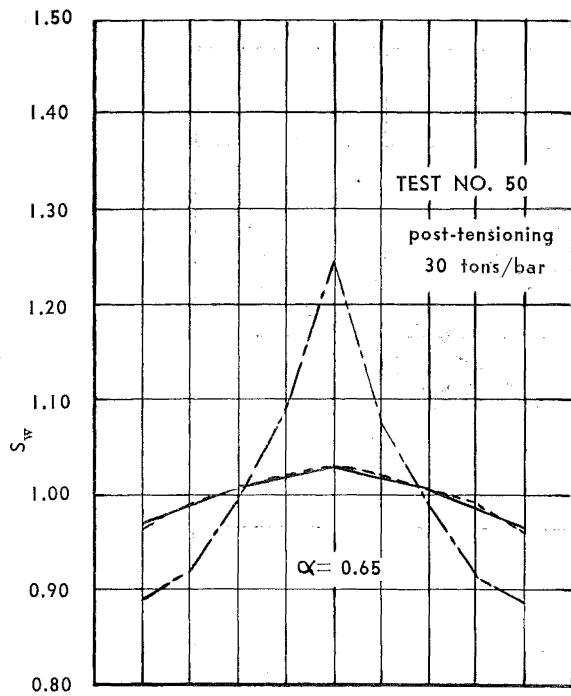$$M_x = - EI_x \frac{\partial^2 w}{\partial x^2}$$

(effect of Poisson's Ratio neglected)

Thus the longitudinal bending moment at each point could be found by differentiating twice the measured longitudinal deflection curve. This method would require a very large number of measuring points and would not be sensitive enough to indicate possible moment concentrations.

More adequate is a consideration of the lateral deflection distribution which, based on the theory of orthotropic plates, can yield the longitudinal bending moments far better than the method mentioned above. First, however, it had to be proven that this theory applies with sufficient accuracy.

For this proof only those tests which fulfilled the basic assumption that no slip occurs between adjacent beams could be

---

* See introduction.

24

TEST NO. 50

post-tensioning
30 tons/bar

$\alpha = 0.65$

TEST NO. 54

no post-
tensioning

$\alpha = 0.08$

CENTER
LOAD

CROSS SECTION

CROSS SECTION

2.358

post-tensioning
30 tons/bar

TEST NO. 60

$\alpha = 0.28$

2.484

no post-
tensioning

TEST NO. 62

$\alpha = 0.10$

EDGE
LOAD

———— MEASURED DEFLECTION COEFFICIENT
- - - - THEORETICAL DEFLECTION COEFFICIENT
—·— MOMENT COEFFICIENTS

FIG. 18
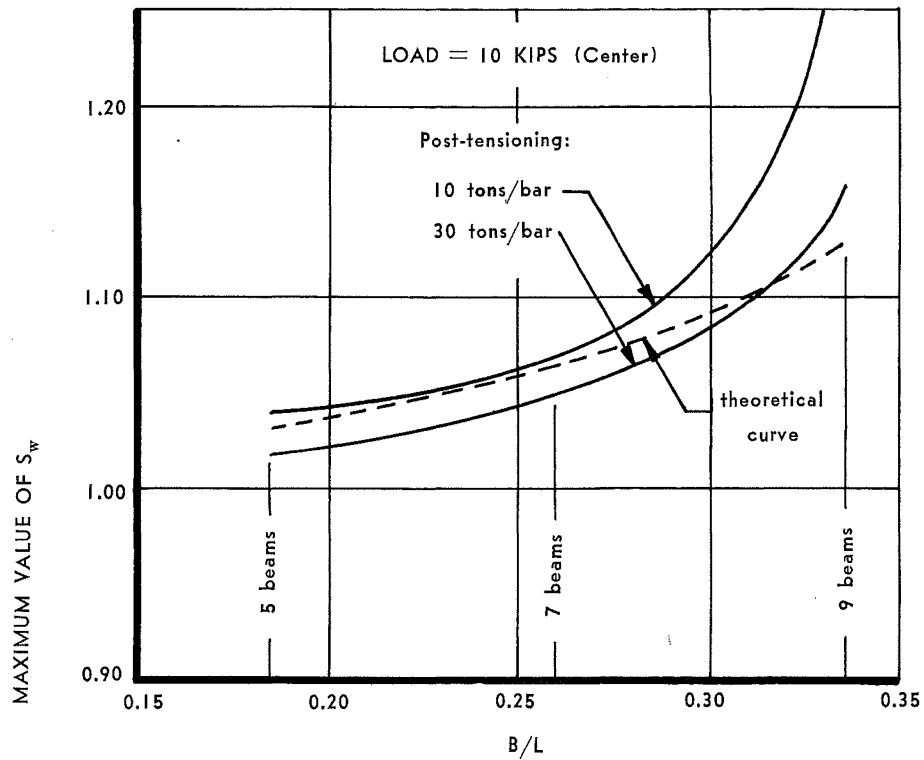THEORETICAL AND MEASURED DEFLECTION DISTRIBUTION
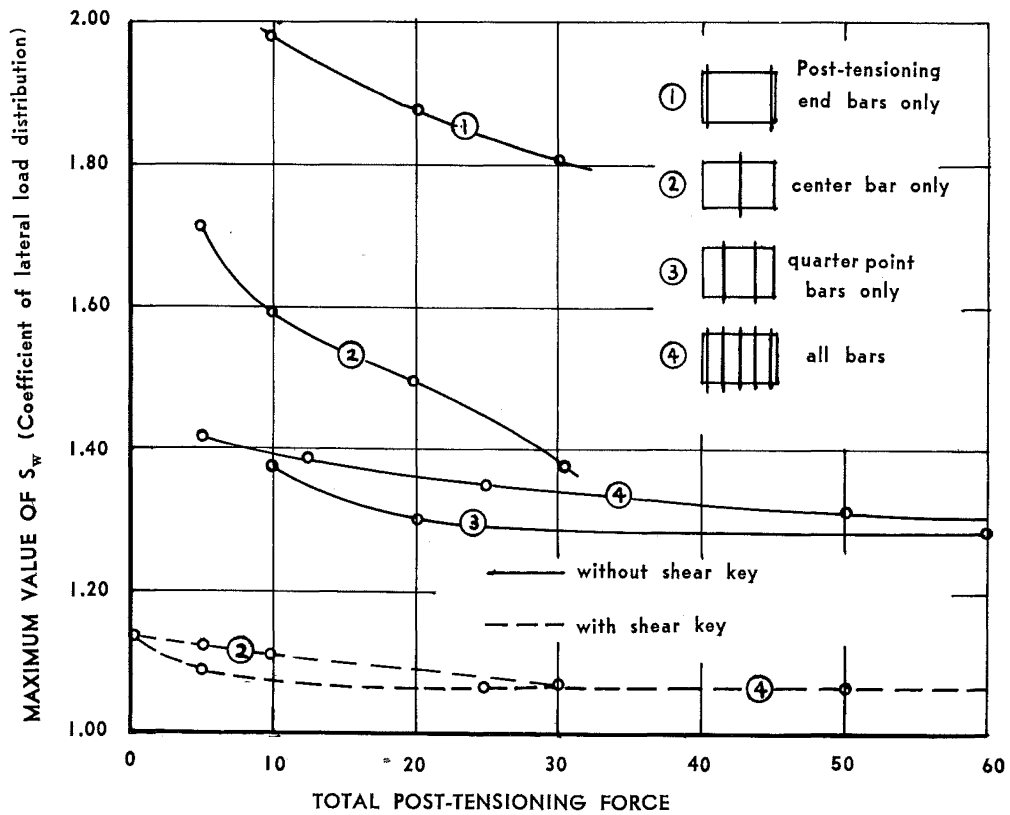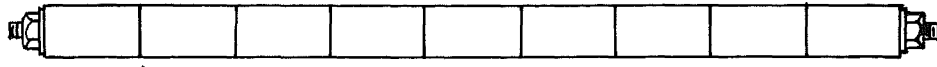
25

FIG. 19

THE INFLUENCE OF THE B/L RATIO

FIG. 20

TOTAL POST-TENSIONING FORCE VS. MAXIMUM VALUE OF s_w

26

CROSS SECTION
TEST #90

DEFLECTION COEFFICIENT

0.80
0.90
1.00
1.10
1.20
1.30

20 K
40 K
80 K
110 K

DEFLECTION COEFFICIENT DISTRIBUTION

DEFLECTION (0.01 in.)

0
40
80
120
160
200
240

20 K
40 K
80 K
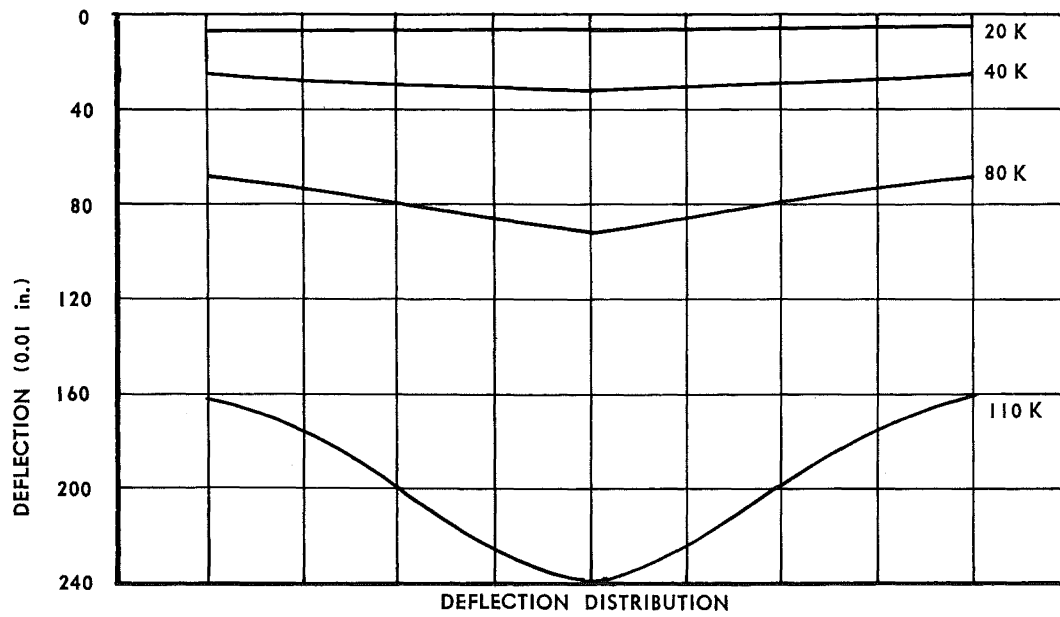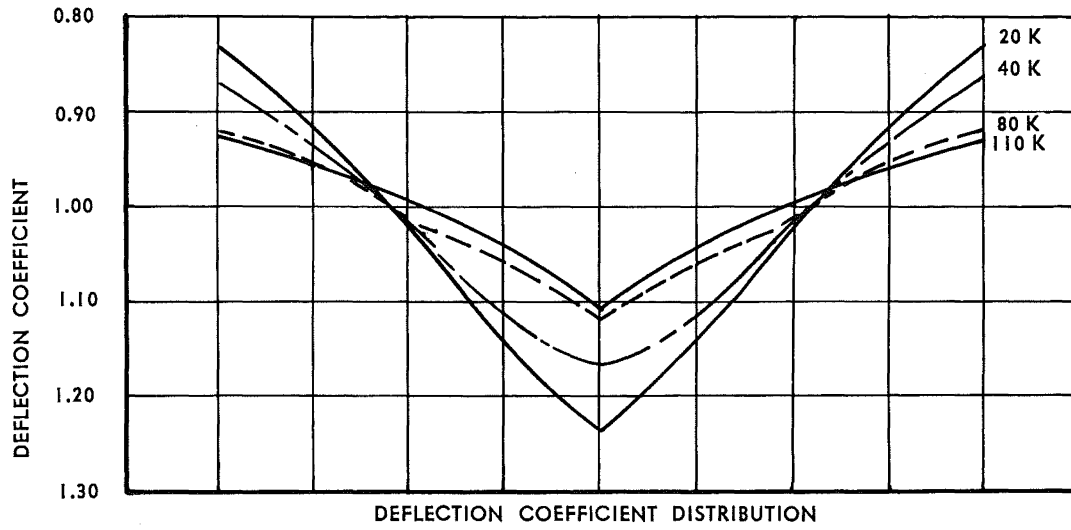110 K

DEFLECTION DISTRIBUTION

FIG. 21

27

considered. This was the case in all tests with grouted shear keys. A certain difficulty developed from the fact that one of the three parameters of the problem, i.e., α, cannot be found by theoretical considerations or by special tests, for reasons explained before. Thus the α values have to be derived from the same tests which serve to check the adaptability of the theory. This means that only the deflected shape, but not the magnitude of the deflections, can be compared for this particular purpose. For this comparison the distribution of the lateral deflection coefficients was calculated as a function of α; the other two parameters, B/L and a/h, are constants for a given bridge. By varying α, the theoretical curve with the same maximum deflection coefficient as the experimental one could be found and the correlation between the distribution of the measured and theoretical coefficients could be checked. Fortunately, the correlation was excellent throughout the test series and it can be concluded that the theory is well applicable as long as no, or only little, slip occurs. This shall be documented with some examples (Fig. 18).

It may be noticed that for the two cases without any post-tensioning α was small but not zero, as expected. When the bridge was disassembled the reason for the latter was found; the grout had adhered so strongly to the beam, that it had provided a considerable lateral bending stiffness.

3. THE INFLUENCE OF THE B/L RATIO

The less the width of a bridge as compared to its length, the better is the lateral load distribution, i.e., the smaller are maximum moment and deflection coefficients.

The relationship between these coefficients and the B/L ratio could be determined from tests 3 to 15, where the width of the bridge was varied by consecutively assembling 5, 7, and 9 beams. In Fig. 19 two typical curves are plotted for post-tensioning forces of 10 and 30 tons per bar, with a load of 10 kips at the bridge center. The devia-

tion of the measured curve from the theoretical is the result of slip, which could not be prevented in these tests without shear keys.

4. THE INFLUENCE OF THE DEGREE AND OF THE LOCATION OF POST-TENSIONING

The maximum moment and deflection are dependent not only upon the degree,* but also upon the location of the lateral post-tensioning. The influence of the latter was studied by post-tensioning four different bar combinations as shown in Fig. 20, where the total post-tensioning force is plotted against the maximum deflection coefficient. The smaller these coefficients are for a given post-tensioning force, the more efficient is the combination. The best load distribution was achieved by post-tensioning only at the quarter points. This is somewhat surprising because, analogous to a gridwork, one might expect post-tensioning of the center bar to give the optimum load distribution. A plausible explanation for the former can be found by considering the different shear characteristic for each case.

A smaller, but still considerable contribution to the lateral load distribution, is obtained by post-tensioning over the supports, which increases the torsional rigidity of the bridge.

From Fig. 20 it can also be concluded that the method often used in practice, i.e., post-tensioning at midspan and over the supports, is fully satisfactory.

5. THE INFLUENCE OF THE MAGNITUDE OF THE LOAD (DESTRUCTION TEST)

Since the lateral bending stiffness of a bridge is dependent upon the magnitude of the applied load, the moment and deflection coefficients cannot remain constant. Only in the case of $\alpha = 1.0$ (isotropic plate), and even then only so long as the resulting

---

* We define the degree of lateral post-tensioning as the total lateral post-tensioning force of the bar divided by the lateral surface of the bridge.

strains stay in the elastic range, are these coefficients independent of the load.

The magnitude and significance of the variation in these deflection coefficients could be observed in the final destruction test (post-tensioning 5 tons at each bar). The measured deflections over the midspan cross-section and the corresponding deflection coefficients are shown in Fig. 21. The variation of the maximum deflection coefficient as a function of the load is plotted in Fig. 22; the irregular shape of this curve was a result of the consecutive cracking of the individual longitudinal beams. It should be noticed that $s_{w\,max.}$ increased only 2.5% in the range from zero load up to cracking of the first beam. The total change in $s_{w\,max.}$ amounted to about 14%.
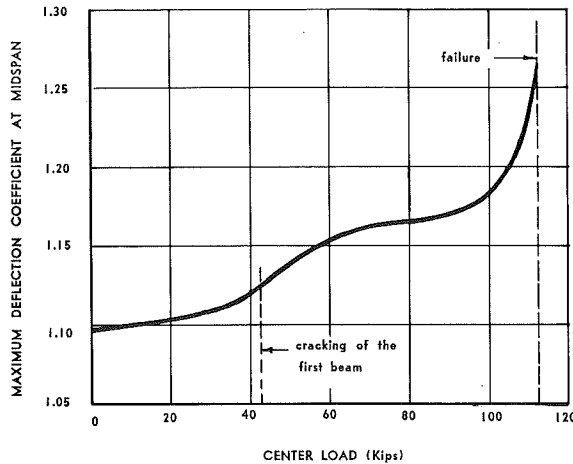

FIG. 22
VARIATION OF MAXIMUM DEFLECTION COEFFICIENT
AS A FUNCTION OF THE LOAD

The bridge finally failed at a load of 113.4 Kips by punching shear (Fig. 23). An underside view of the bridge after destruction is presented in Fig. 24. Of special in-terest is the fact that the ultimate capacity of the bridge was only 4 percent smaller than the sum of the ultimate capacities of all the beams. This means that for an actual bridge, where such load concentrations are impossible, the ultimate capacity of the entire structure can be obtained by adding the capacities of all the members.

6. THE LONGITUDINAL BENDING MOMENTS

   a. Complete interaction of the shear keys and no development of slip

In Section 2 of Chapter B it is explained why the distribution curves of the deflection coefficients do not coincide with the distribution curves of the moment coefficients. The conversion from one to the other needs a theoretical relationship, in our case the theory of orthotropic plates. The values of the coefficients for the measured deflections and for the calculated longitudinal bending moments are presented in Tables 2a-2f. The latter were found by the following proced-ure: first, the α value was determined by comparing the measured with the theoretical maximum deflection coefficient. Since α, B/L and a/h were then known, the actual longitudinal bending moments of each beam could be calculated.

   b. With slip and incomplete interaction of the shear keys

Under these conditions no direct correla-tion between the theory and the test results exists. In order to estimate the longitudinal bending moments for each beam, necessary for the design, a method had to be estab-
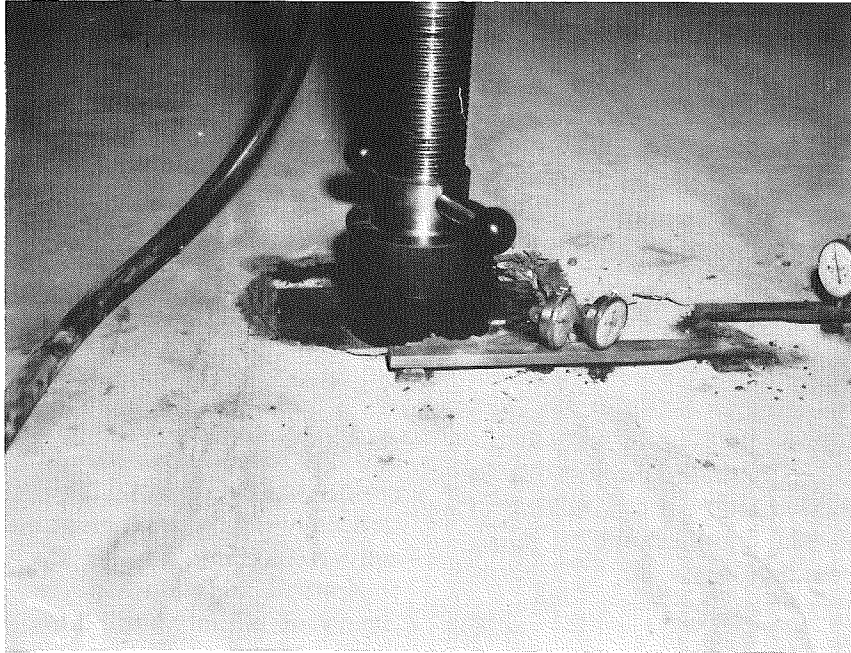
FIG. 23
DESTRUCTION OF THE BRIDGE BY PUNCHING SHEAR

FIG. 24
UNDERSIDE VIEW OF THE BRIDGE AFTER FAILURE

lished to approximate these moments such that they are always on the safe side. This method is based on the following assumption: the slip does not change the lateral bending stiffness of the bridge. This means that the deflection of a lateral strip is considered to consist of two separate phenomena —one is a continuous rotation of the strip elements (i.e., simple bending), the other is a discontinuous vertical displacement of some strip segments (a strip segment = a cross-section of an individual beam). The action of the plate, therefore, can also be imagined to consist of two separate phases: in the first, the bridge deflects as a normal orthotropic plate (plate bending), in the second, caused by slip, the longitudinal beams deflect individually without torsion (additional beam bending). The additional beam bending can be positive or negative depending upon the proximity to the load. The longitudinal bending moments resulting from the plate bending follow the same rules used so far. The change, percentage-wise, in these bending moments is considered to be proportional to the change, percentage-wise, in the

deflection due to slip. Expressed in terms of coefficients, this becomes

$$S_{M_s} = \frac{s_M}{s_w} \cdot s_{W_s}$$

$s_{M_s} =$ moment coefficient with slip
$s_M =$ moment coefficient without slip
$s_{W_s} =$ deflection coefficient with slip (measured)
$s_w =$ deflection coefficient without slip (measured)

It can be proved that this method always over-estimates the maximum bending moment and is, therefore, satisfactory for design purposes.

7. EMPIRICAL FORMULAS

a. The Parameter

Since the theoretical prediction of α seems to be impossible, an attempt was made to find a method for its approximation. Hence, empirical formulas were developed in terms of the post-tensioning and the load.
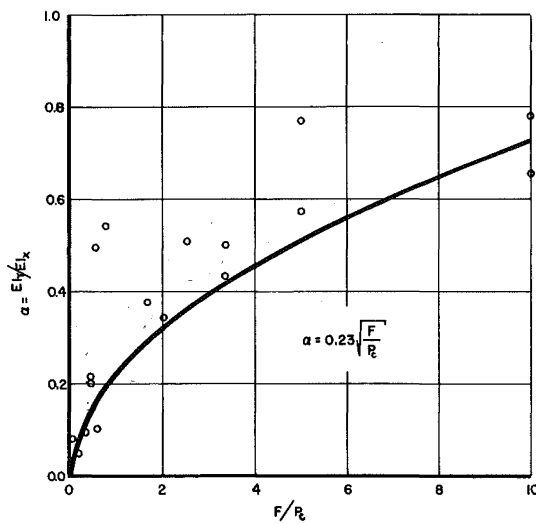

FIG. 25
RELATIONSHIP BETWEEN α AND
(center load)

$$\alpha = \frac{EI_x}{EI_y} = \frac{\text{Lateral bending stiffness}}{\text{Longitudinal bending stiffness}}$$

$$\frac{F}{P_c} = \frac{\text{Total post-tensioning force}}{\text{Applied center load}}$$
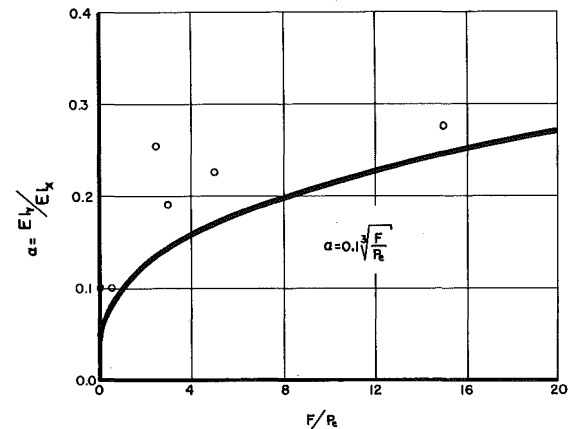

FIG. 26
RELATIONSHIP BETWEEN α AND
(edge load)

$$\alpha = \frac{EI_x}{EI_y} = \frac{\text{Lateral bending stiffness}}{\text{Longitudinal bending stiffness}}$$

$$\frac{F}{P_e} = \frac{\text{Total post-tensioning force}}{\text{Applied edge load}}$$

31

For these formulas, all details such as the number or location of the post-tensioning bars were neglected; only the total post-tensioning force was considered, excluding that case where only bars over the supports are provided. Center and edge loading yielded different formulas, namely:

$$\text{Center load:} \quad \alpha = 0.23 \sqrt[2]{\frac{F}{P_c}}$$

$$\text{Edge load:} \quad \alpha = 0.10 \sqrt[3]{\frac{F}{P_e}}$$

The points resulting from our tests and the curves given by these formulas (chosen to be a lower boundary of the test points) are shown in Fig. 25 and Fig. 26. If a bridge is subjected to a load resulting from several trucks, P (center or edge) is not the total load, but only the portion concentrated at the peak of the moment coefficient curve. This means, for most practical cases, that the applied center load (P_c) is equal to two

wheel loads, whereas the applied edge load (P_e) is usually equal to one wheel load.

b. The increase in moment coefficient due to slip and incomplete interaction of the shear keys

It was felt that a suitable way of taking into account the effect of slip and incomplete interaction of the shear keys was to increase the value of the maximum moment coefficient. This increase (in per cent) versus F/P was plotted as an upper boundary to the test points for the two cases — with and without shear keys (Fig. 27). Since the shear keys of our laboratory bridge were stronger than those found in practice, the results of a field test* on a bridge with normal shear keys were also included to find the lower curve of Fig. 27.

———

* A. Roesli, C. E. Ekberg, Jr., A. Smislova, W. J. Eney "Field Tests on a Prestressed Concrete Multi-Beam Bridge" (Progress Report 9).
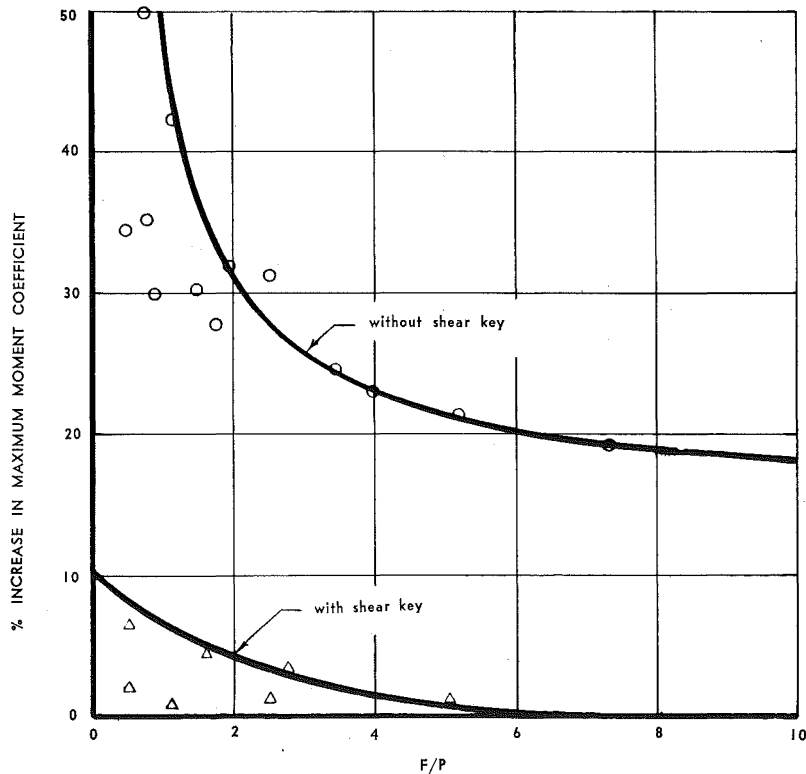

FIG. 27

INCREASE (per cent) IN MOMENT CO-EFFICIENT DUE TO SLIP AND INCOMPLETE INTERACTION OF SHEAR KEY (center or edge load)

$$\frac{F}{P} = \frac{\text{Total post-tensioning force}}{\text{applied edge or center load}}$$

E. CONCLUSIONS AND RECOMMENDATIONS

(1)

The theory of orthotropic plates, as established in Progress Report 10*, was found to be well applicable to the analysis of multibeam bridges. The correlation between the results of the theory and those of the tests was very close as long as only little displacement developed between adjacent beams.

(2)

When the relative displacement between adjacent beams becomes decisive, the theory of orthotropic plates may still be used, however an empirical modification is necessary.

(3)

The theoretical relationship between α (coefficient of the bending stiffnesses) and β (coefficient of torsional rigidity) established in Progress Report 10* was confirmed by our tests. This means that the influence of the torsional rigidity of the bridge can be expressed in the final solution by the parameter a/h (width of beam/depth of beam).

The design of a multibeam bridge is mainly governed by the longitudinal bending moments. Two load conditions can be critical: either a load concentration at the center of the bridge or at midspan of an edge beam. The maximum s_M value† (coefficient of longitudinal bending moment) for a given bridge is always higher for edge loading than for center loading, but since in the latter the possible load concentration is larger, the critical bending moment may occur in the center beam. Therefore, both load conditions have to be checked.

(5)

Shear can be critical either by punching through of a wheel load or in diagonal tension in an individual beam. The factor of safety against punching shear may be ascertained in the usual manner. The diagonal tension stresses may be calculated approximately by subjecting an individual beam to a certain fraction of wheel loads. It is safe to take the same fraction as derived for bending.

(6)

No factor of safety should be required for uncertainties in the lateral load distribution as such for the following reason:

An error in estimating α produces a decisive change in the maximum moment coefficient. Fortunately, the maximum longitudinal bending moment resulting from a superposition of all load influences is less sensitive to errors in α. In Fig. 28 the maximum moment coefficient of a bridge and its maximum longitudinal bending moments under a four lane loading are plotted as a function of α, taking both moment and coefficient arbitrarily as 100% for $\alpha = 1$. While the maximum moment coefficient varies about 80% over the entire range of
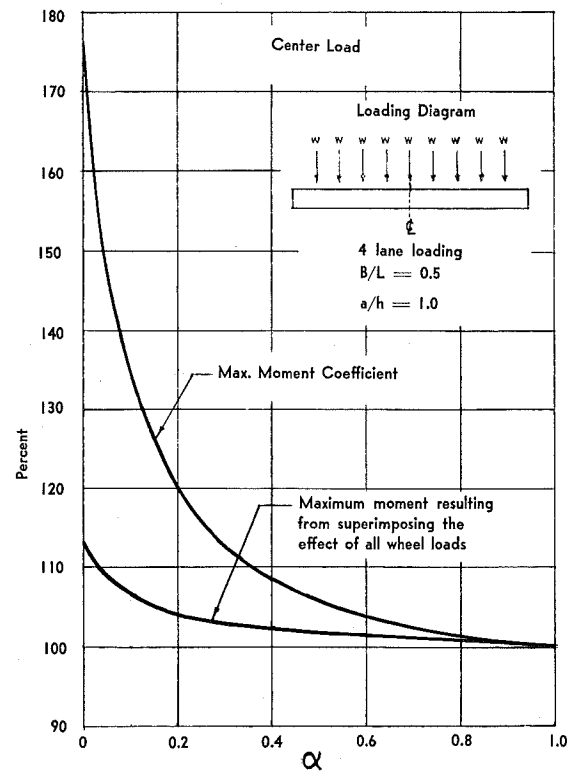

FIG. 28

---

* See introduction.
† The definition and application of these moment coefficients are given in the Résumé of the Analysis of Multi-Beam Bridges.

α (from zero to one), the maximum moment increases only by 12% (for edge loading only 8%).

(7)

The ultimate capacity of a prestressed multi-beam bridge of normal construction can be expected to closely approach the sum of the capacities of all the members, provided that no punching shear failure occurs.

(8)

From (6) and (7) it follows that the safety of a multi-beam bridge can be guaranteed if:

(a) the individual beams under the loads derived from the theory of lateral load distribution fulfill all the requirements of the specifications.

(b) that the punching shear stresses under a wheel load do not exceed the allowable limits.

(9)

For the calculation of α (ratio of lateral to longitudinal bending stiffness) empirical formulas were derived from our tests as a function of F/P (total post-tensioning force/applied concentrated load). A distinction between center and edge loading must be made.

$$\text{Center loading:} \quad \alpha = 0.23 \sqrt[2]{\frac{F}{P_c}}$$

$$\text{Edge loading:} \quad \alpha = 0.10 \sqrt[3]{\frac{F}{P_e}}$$

These α values are conservative, as can be seen in Fig. 25 and Fig. 26.

(10)

The influence of slip and incomplete interaction of the shear keys can be considered by increasing the maximum moment coefficient, s_M, as shown in Fig. 27. The points indicating test results were found from this investigation as well as from a field test.* Again the empirical curves are chosen such that the obtained bending moments are on the conservative side.

(11)

A good lateral load distribution of a geometrically given bridge is dependent upon the effectiveness of post-tensioning and shear transfer between adjacent beams. The predominant influence is that of strong shear keys. The question of when it is economical to apply post-tensioning can be judged from case to case by making use of the various charts given in this report.

(12)

If post-tensioning is provided, care has to be taken to prevent the beams from cracking laterally. The beams are always a bit warped with respect to a vertical longitudinal plane, due to the unequal pretensioning of the longitudinal tendons. The lateral post-tensioning tends to straighten the beams; this can cause lateral cracks across the sides of the beams. In order to prevent such cracks, grouted bearing areas should be provided between all beams at the location of the post-tensioning bars.

(13)

Among various combinations of post-tensioning, the greatest efficiency is attained by arranging the bars either at the quarter points or by distributing them over the entire bridge. A relatively high efficiency may also be obtained by providing bars over the supports and at midspan, as might be more practical in the field.

---

* See introduction.

F. RÉSUMÉ OF THE ANALYSIS OF MULTI-BEAM BRIDGES

The purposes of this chapter are to briefly explain the analysis of multi-beam bridges according to the theory of orthotropic plates and to give all the formulas and charts necessary for their design. Only results and recommendations on the procedure are reported; for all the details or reasoning we refer to the preceeding chapters and to Progress Reports 9 and 10.* The numerical solutions of the partial differential equation of orthotropic plates were all taken from the theoretical study by A. Roesli.*

Due to all these investigations the design of multi-beam bridges becomes rather straightforward. It is essentially reduced to the problem of how to load an individual beam such that the resulting maximum of the critical internal forces is equal to their maximum in the bridge. The critical internal force is usually the longitudinal bending moment, which can be calculated if the lateral distribution of the longitudinal bending moments is known. This shall be explained more extensively.

Since the bridge is a plate, simply supported along two opposite edges, the calculation of the total bending moment of a lateral bridge cross-section is a statically determinate problem, identical to that of a single beam. This total bending moment, divided by the width of the bridge, represents the average bending moment of the cross-section ($M_{x\,av}$). The actual bending moment per unit width at each point in the cross-section can be expressed as a proportion of $M_{x\,av}$. The factor of proportionality of each point is, by definition, the coefficient of the longitudinal bending moment (s_M).

$$s_M = \frac{M_x}{M_{x\,av}}$$

The essential part of the analysis is the determination of the distribution over a cross-section of these dimensionless coefficients. As will be seen later, two distribution curves may be of concern: one for a load concentration at bridge center, the other for a load concentration at midspan of an edge beam.

The distribution of the moment coefficients is dependent on three parameters:

$$\frac{B}{L} = \frac{\text{half width of bridge}}{\text{length of bridge}}$$

$$\frac{a}{h} = \frac{\text{width of single beam}}{\text{depth of single beam}}$$

$$\alpha = \frac{\text{lateral bending stiffness}}{\text{longitudinal bending stiffness}}$$

B/L and a/h are merely geometrical properties of the bridge, whereas α may be calculated by the empirical formulas:

Center loading: $\alpha = 0.23\sqrt[2]{\dfrac{F}{P_c}}$

Edge loading: $\alpha = 0.10\sqrt[3]{\dfrac{F}{P_e}}$

F = total post-tensioning force
P_c = applied concentrated load at bridge center
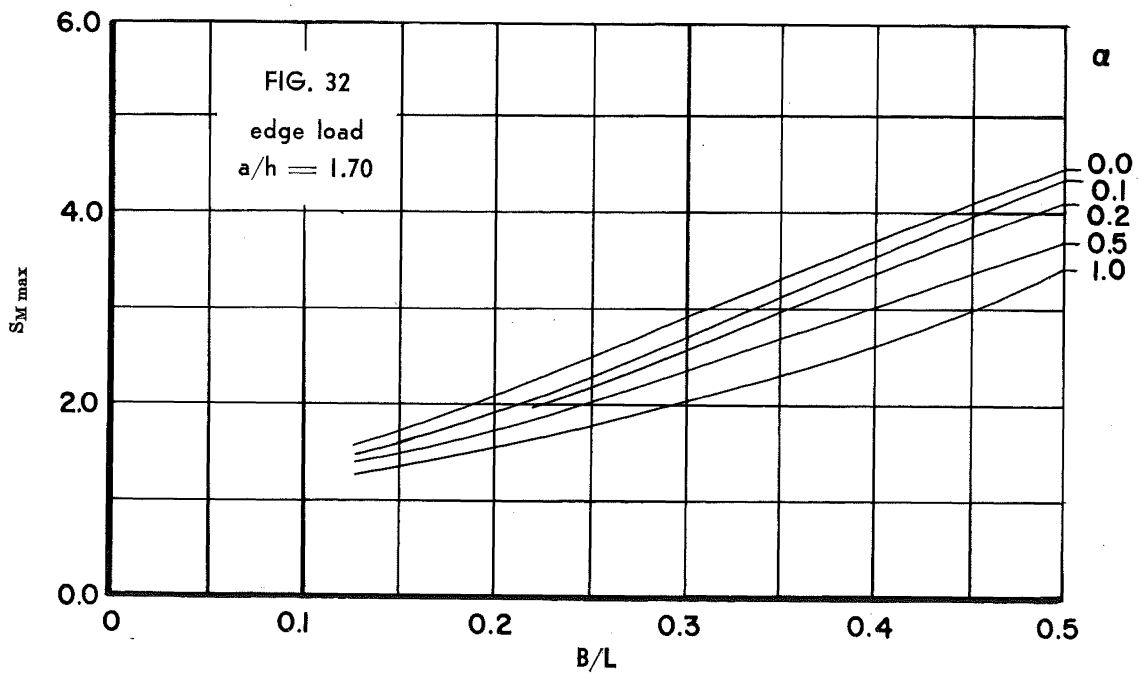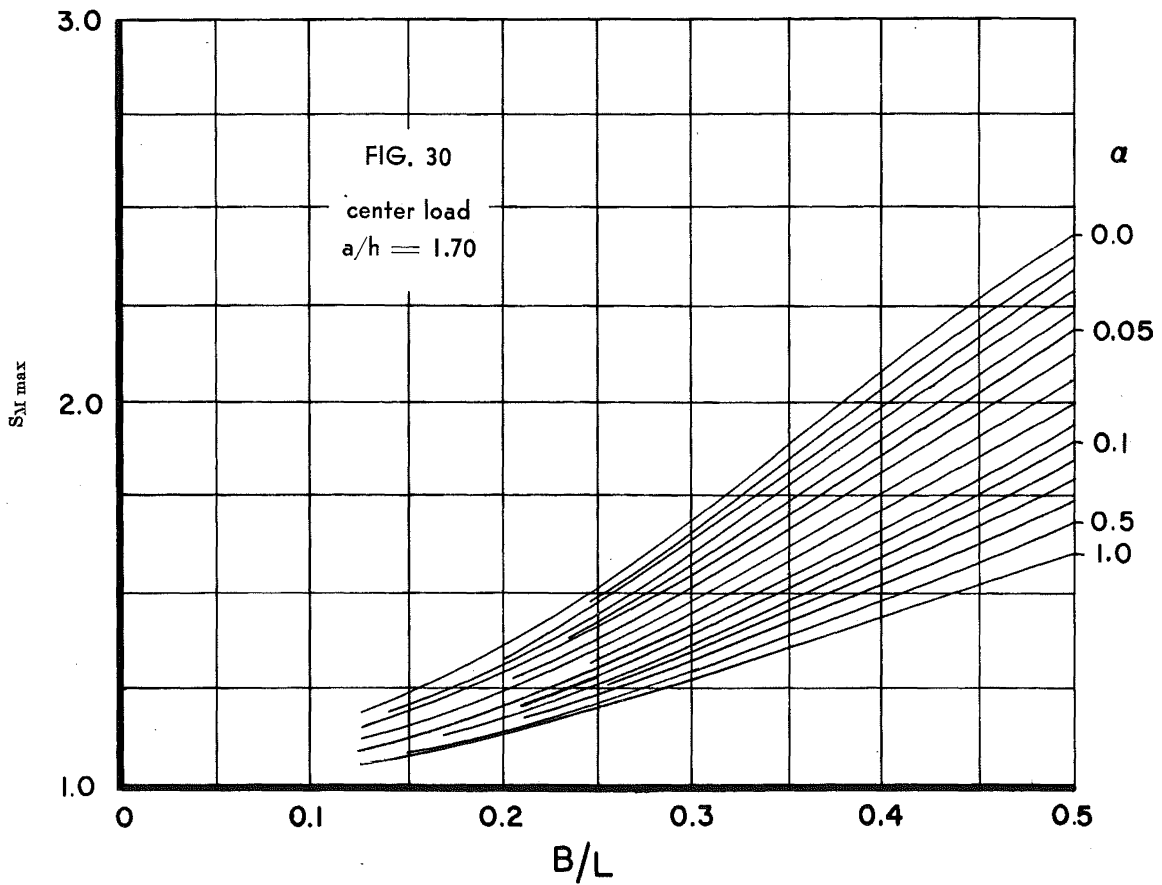P_e = applied concentrated load at midspan of an edge beam

If a bridge is subjected to a load resulting from several trucks, P_c and P_e do not represent the total load, but only the portion concentrated at the peak of the moment coefficient curve. This means, for most of the practical cases, that the applied center load (P_c) is equal to two wheel loads, whereas the applied edge load (P_e) is usually equal to one wheel load.

In comparing the solutions of the theory of orthotropic plates, it was found that the distribution curve can be considered as dependent on $s_{M\,max}$ only; no matter from what combination of B/L, a/h and α this $s_{M\,max}$ may result. Hence the distribution curve is known if $s_{M\,max}$ is known. The value of $s_{M\,max}$, dependent upon a/h, B/L and α, is given in Figs. 29 to 32. Linear interpolation

---

* See introduction.

35
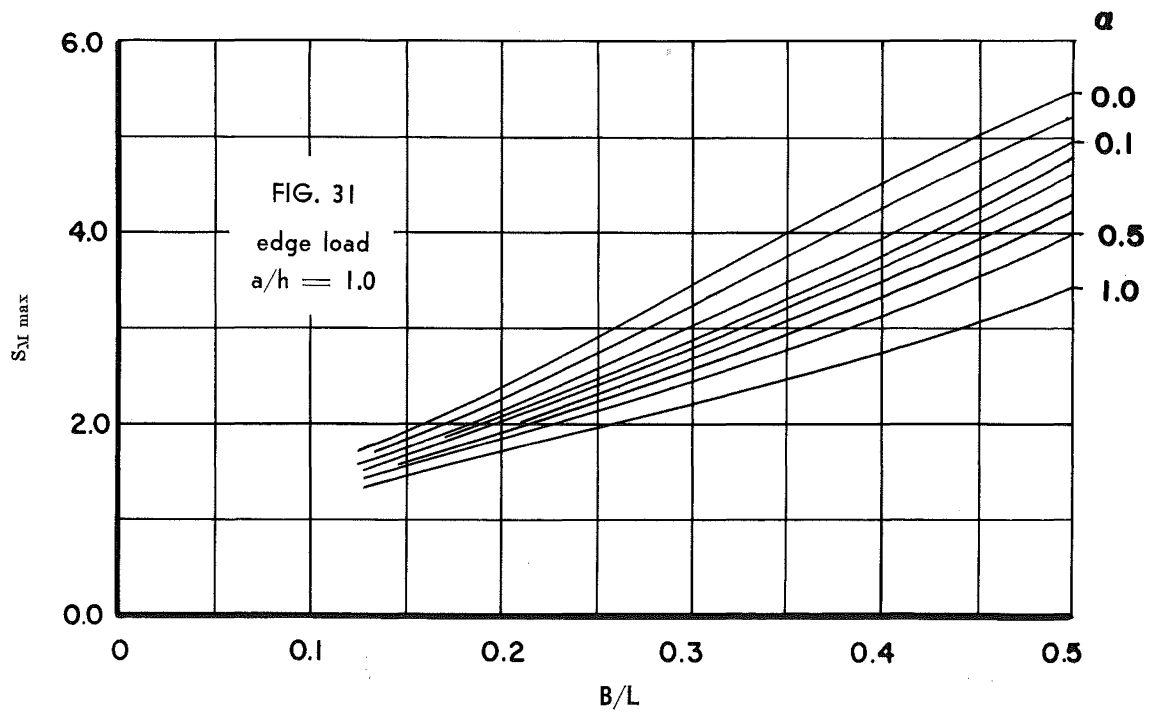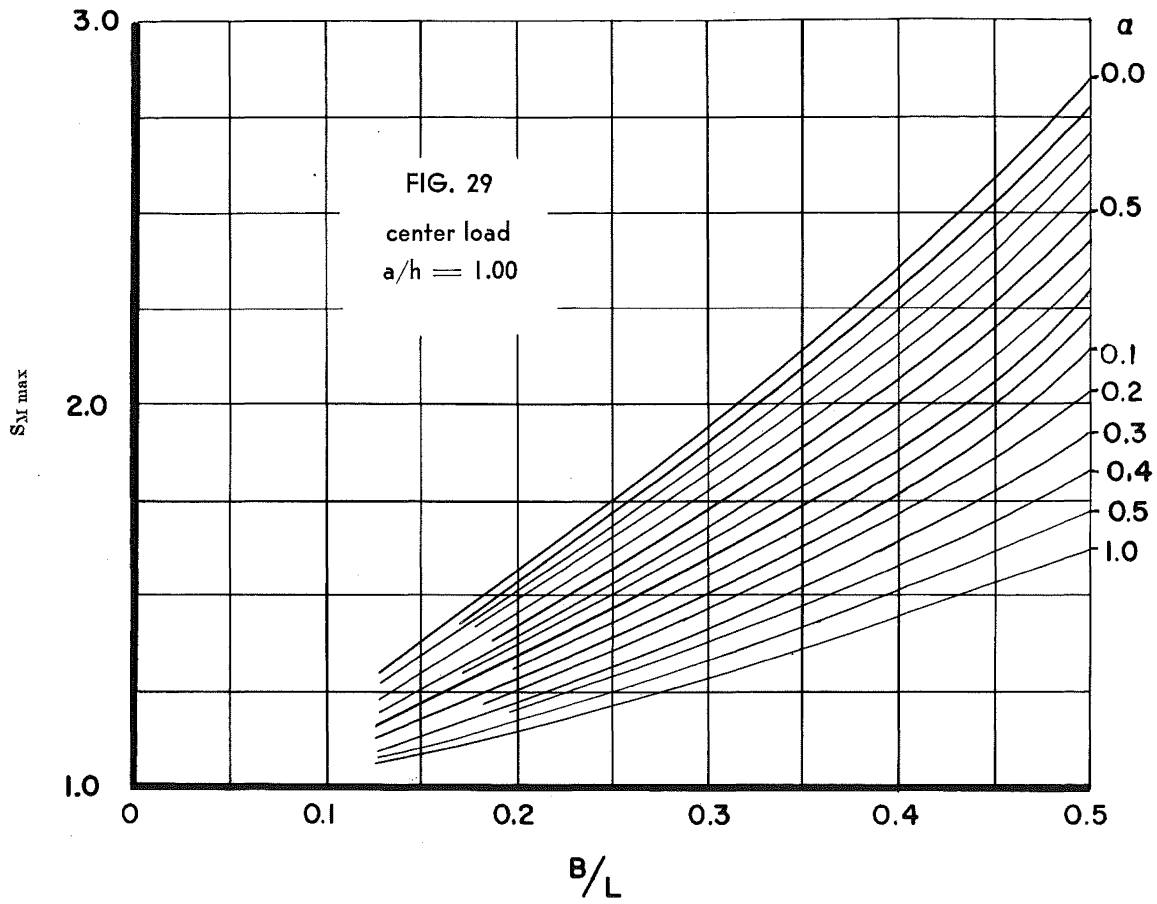
Maximum values of s_M coefficient of lateral moment distribution) as a function of the parameters α, B/L, a/h and the location of the concentrated load.

FIG. 30

center load

a/h = 1.70

α

0.0

0.05

0.1

0.5

1.0

$S_{M\ max}$

B/L

FIG. 32

edge load

a/h = 1.70

α

0.0
0.1
0.2
0.5
1.0

$S_{M\ max}$

B/L

Legend: B = 1/2 Width of bridge

L = Length of bridge

$\alpha = \dfrac{EI_y}{EI_x} = \dfrac{\text{Lateral bending stiffness}}{\text{Longitudinal bending stiffness}}$

$a/h = \dfrac{\text{Width of single beam}}{\text{Depth of single beam}}$

FIG. 33

38

Distribution of moment coefficients for center load

COEFFICIENT OF LATERAL MOMENT DISTRIBUTION

DISTANCE FROM CENTER

Distribution of moment coefficients for edge load

FIG. 34

COEFFICIENT OF LATERAL LOAD DISTRIBUTION

DISTANCE FROM CENTER

39

BRIDGE CROSS-SECTION

W_n

wheel load

b_n

a

2B

F_n

s_M
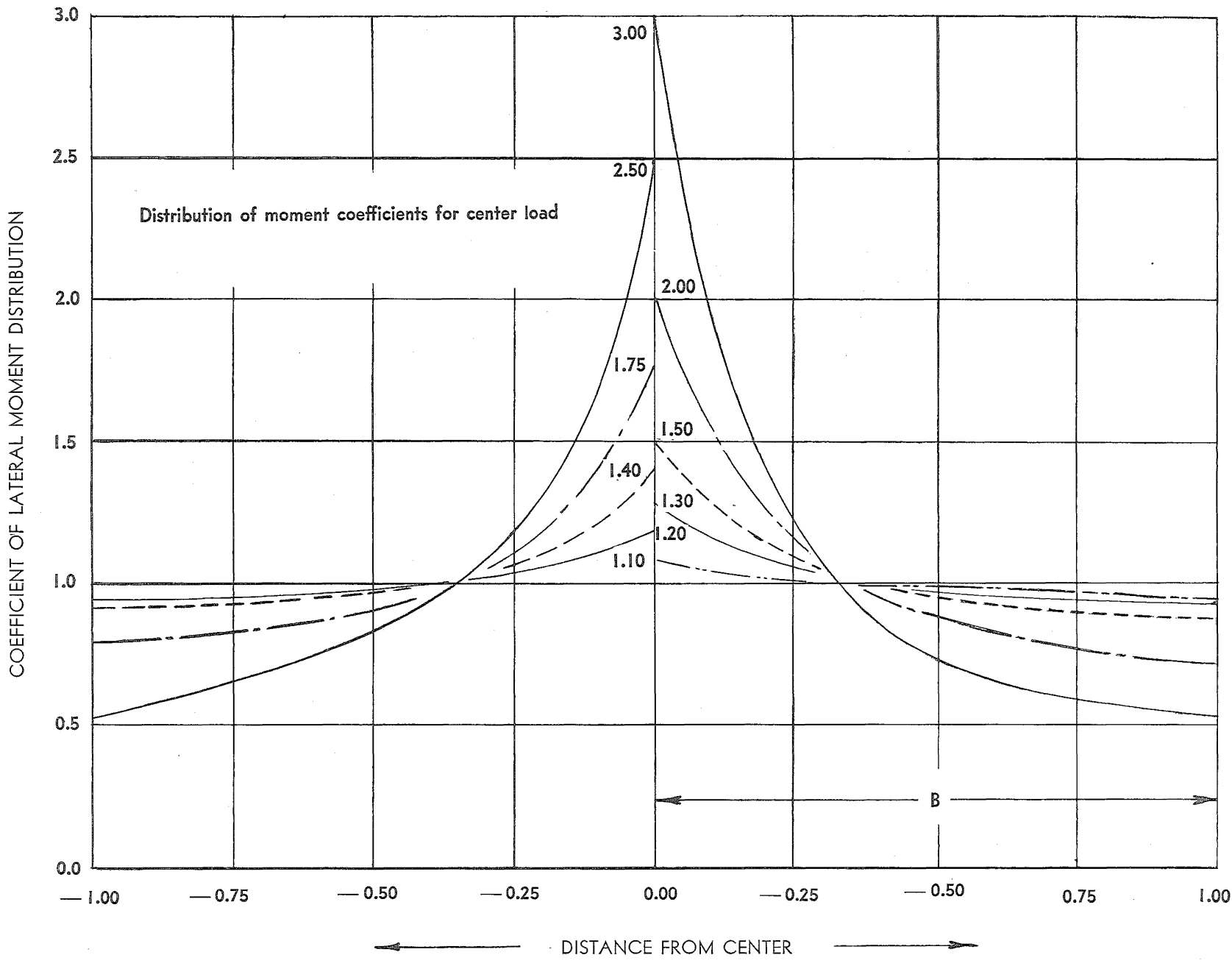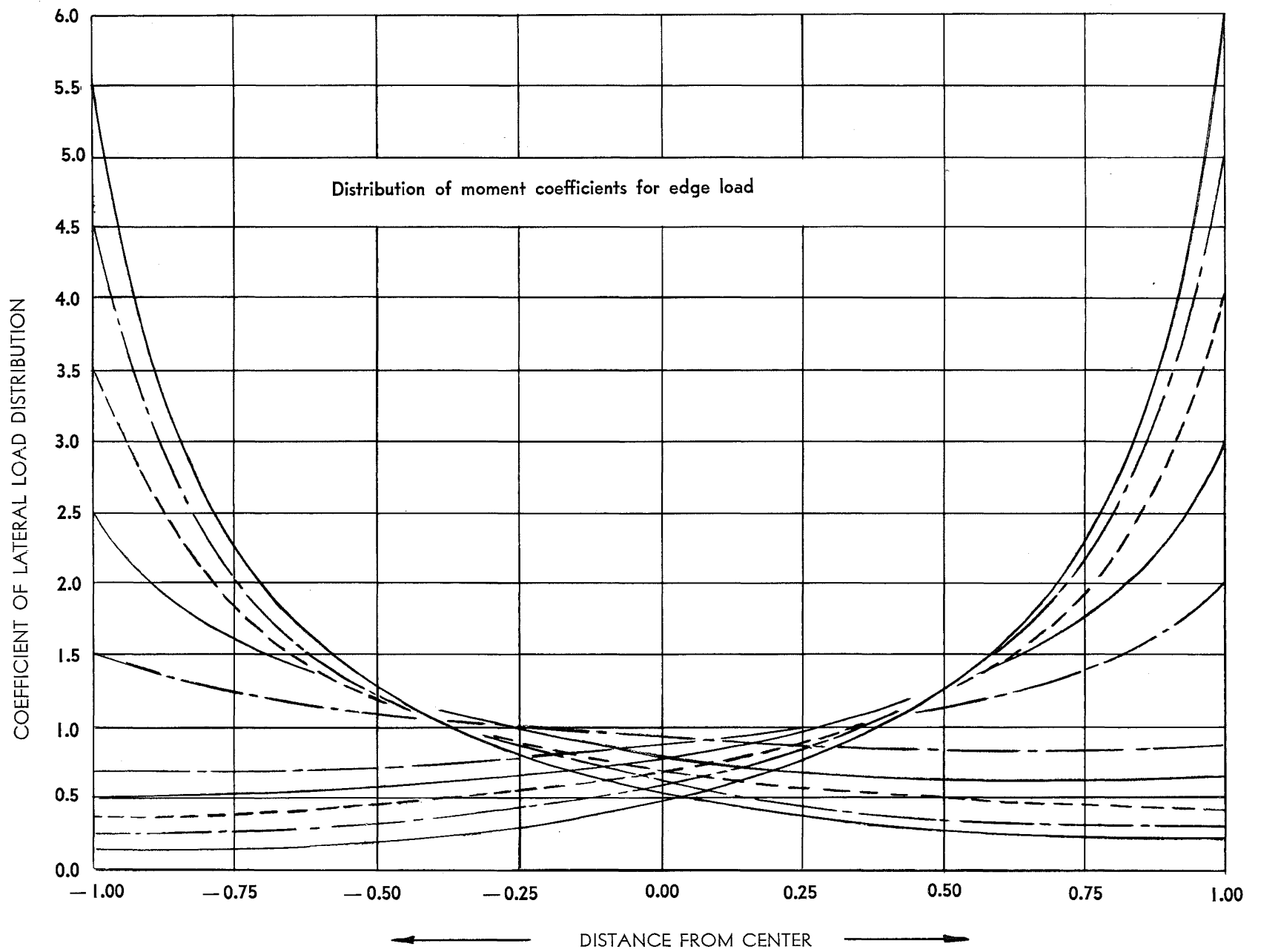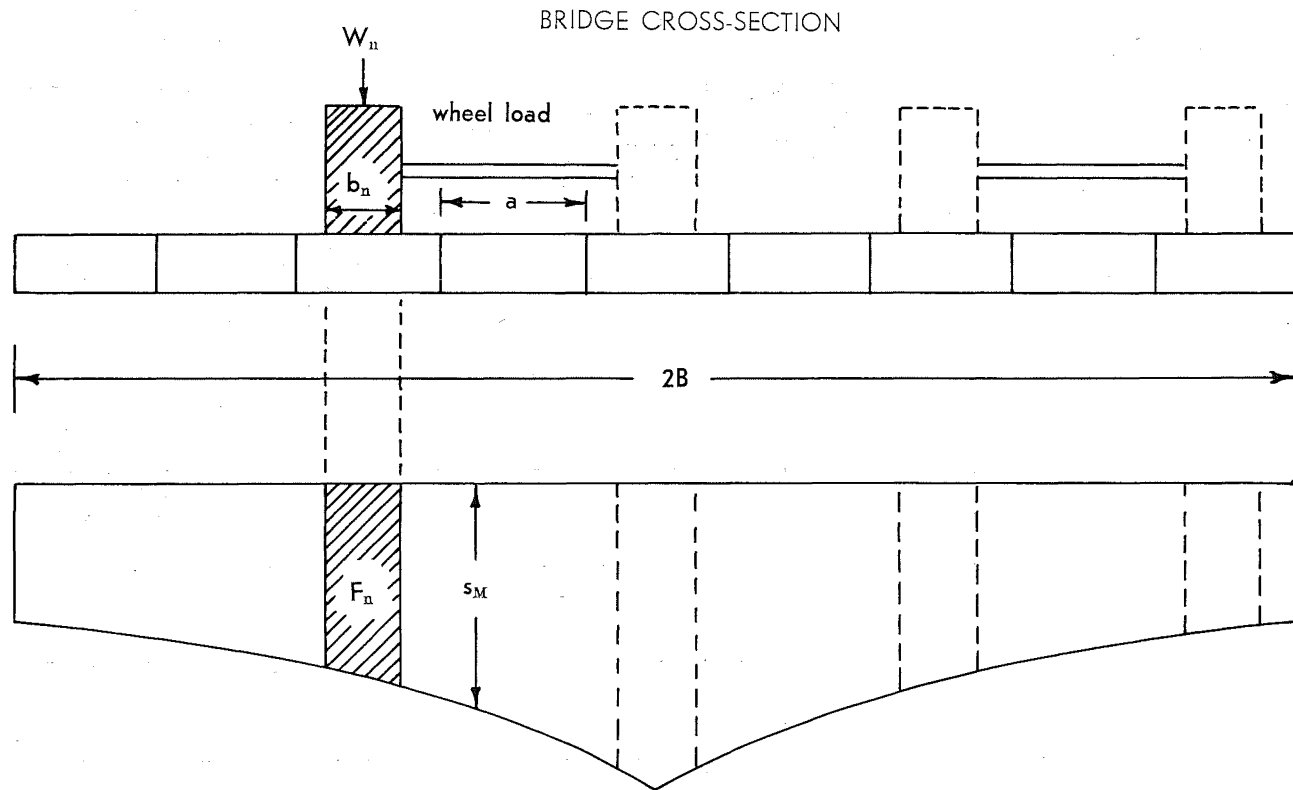
FIG. 35

EVALUATION OF THE MAXIMUM MOMENT

Distribution curve of the coefficients of the longitudinal bending moments (s_M) = influence line for the longitudinal bending moment of the center beam.

or extrapolation will be necessary if a/h is not equal to either 1.0 or 1.7.

If no, or only a small, post-tensioning is provided, $s_{M\,max}$ has to be increased, to compensate for slip or incomplete interaction of the shear keys. Fig. 27 indicates how large this percentage increase should be made. Again, P is not the total load but only the largest possible load concentration.

Once the maximum value for s_M is calculated in this manner, the distribution curve can be taken from Fig. 33 and Fig. 34 for center and edge load respectively. These distribution curves can also be considered as influence lines for the longitudinal bending moments.

The influence of a wheel load (W_n) of the width b on the moment at the center of a given cross-section (Fig. 35) can be expressed as:

$$M_n = \frac{F_n}{b_n} \cdot M_{n\,av}$$

$M_{n\,av}$ is the average moment of the cross-section due to W_n alone and can be written in the form:

$$M_{n\,av} = k \cdot \frac{W_n}{2B}$$

where k is a constant depending only upon the length of the bridge and the location of the cross-section.

If the bridge is subjected to a number of n different wheel loads the moment becomes:

$$M = \sum_o^n M_n = \sum_o^n \left(\frac{F_n}{b_n} \cdot M_{n\,av} \right)$$

$$= \frac{k}{2B} \sum_o^n \left(\frac{F_n}{b_n} \cdot W_n \right)$$

In order to design an individual beam we have to find an equivalent load (W_{eq}) which, applied to the beam, would produce the same moment M as is present in the bridge; i.e.:

$$M_{eq.} = k \cdot \frac{W_{eq.}}{a} = M$$

Thus:

$$W_{eq.} = \frac{a}{2B} \cdot \sum_o^n \left(\frac{F_n}{b_n} \cdot W_n \right)$$

Since $\dfrac{2B}{a}$ represents the number of beams (m), the formula becomes:

$$W_{eq.} = \frac{1}{m} \cdot \sum_o^n \left(\frac{F_n}{b_n} \cdot W_n \right)$$

In most of the practical cases, all the wheel loads in one cross-section are equal and the area (F_n) under the curve approximates that of a trapezoid. This simplifies the formula to

$$W_{eq.} = W_n \cdot \frac{\sum^n s_M}{m}$$

$W_n =$ one wheel load
$m =$ number of beams
$n =$ number of wheel loads over one cross-section

The lateral moment distribution is least uniform at midspan; this means that W_{eq} becomes greatest at the midspan cross-section. If the above ratio W_{eq}/W_n is used as a reduction factor for all the loads along one beam, the resulting design is conservative. Thus the final step is to design a single beam under critical wheel load combinations, where each wheel load may be reduced by the ratio W_{eq}/W_n. Although this reduction factor was derived for bending, it may also be used to calculate the diagonal tension stresses of an individual beam.

To illustrate this method a typical example is presented:

41

Example

GIVEN:

    Width of the bridge = 4 lanes   Length of the bridge = 60 feet

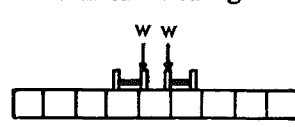   A. A. S. H. O. Specifications   Loading = H20-S16-44

CHOSEN:

    Post-tensioning = 3-⅝" bars; working force/bar = 26,050 lbs.

    Assumed cross-section = 36" x 36"

    Shear keys will be used

    Center lanes = 13 feet; Outside lanes = 12.5 feet
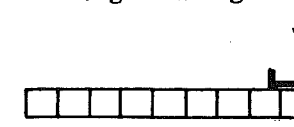
CALCULATIONS:

1. Determination of α :

center loading   edge loading

$P_c = 32,000$ lbs. $P_e = 16,000$ lbs.

$$\frac{F}{P_c} = \frac{26{,}050 \cdot 3}{32{,}000} = 2.44 \qquad\qquad \frac{F}{P_e} = \frac{26{,}050 \cdot 3}{16{,}000} = 4.88$$

$$\alpha = 0.36 \qquad\qquad\qquad\qquad \alpha = 0.17$$

$$\frac{F}{P} = \frac{\text{total post-tensioning force}}{\text{maximum concentrated load}}$$

α may be read directly from Figures 25 and 26:

2. Determination of the maximum coefficient of lateral moment distribution.

$$\frac{a}{h} = \frac{\text{width of the beam}}{\text{depth of the beam}} = \frac{36''}{36''} = 1$$

$$\frac{B}{L} = \frac{\text{half the bridge width}}{\text{length of the bridge}} = \frac{51/2}{60} = 0.43$$

The coefficient of lateral moment distribution for center loading, independent of slip, may not be read directly from Fig. 29. If a/h was between 1.0 and 1.7, it would then have been necessary to interpolate between Fig. 29 and Fig. 30. Figures 31 and 32 are used in the same manner to determine the coefficient for the edge load. From Fig. 27 we may estimate the effect of the slip and incomplete interaction of the shear keys.

From 29: $s_M = 1.67$ From 31: $s_M = 4.10$

From Fig. 27 — 3.5% increase   From Fig. 27 — 1.3% increase

s_M total = 1.67 + 0.035 (1.67) = 1.73 s_M total = 4.10 + 0.013 (4.10) = 4.15

3. Final lateral moment distribution curves:

From figures 33 and 34 the desired curves are interpolated. These curves are also the influence lines for the longitudinal bending moments. To determine the effect of several loads, we shall load the influence lines. The percentage of wheel load which is to be carried by one beam is then $\geq s_M/m$:
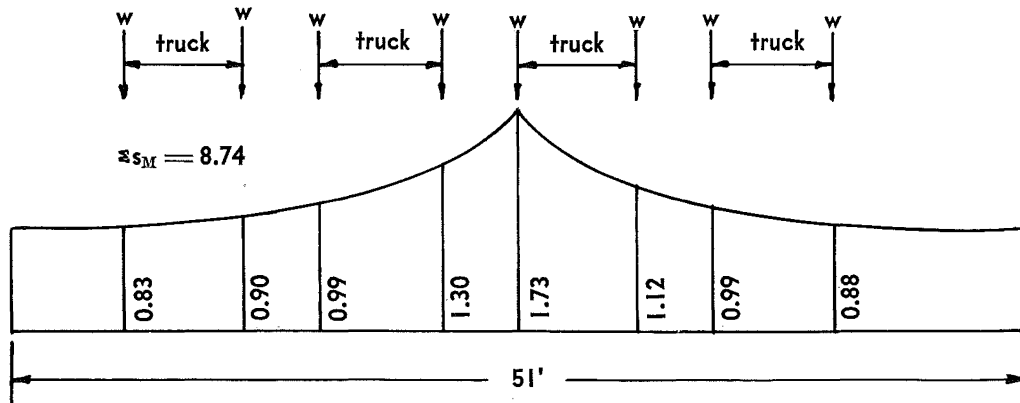
$$\frac{W_{eq.}}{W} = \frac{\geq s_M}{m} = \frac{\text{Summation of the coefficients}}{\text{number of beams}}$$

Center loading:
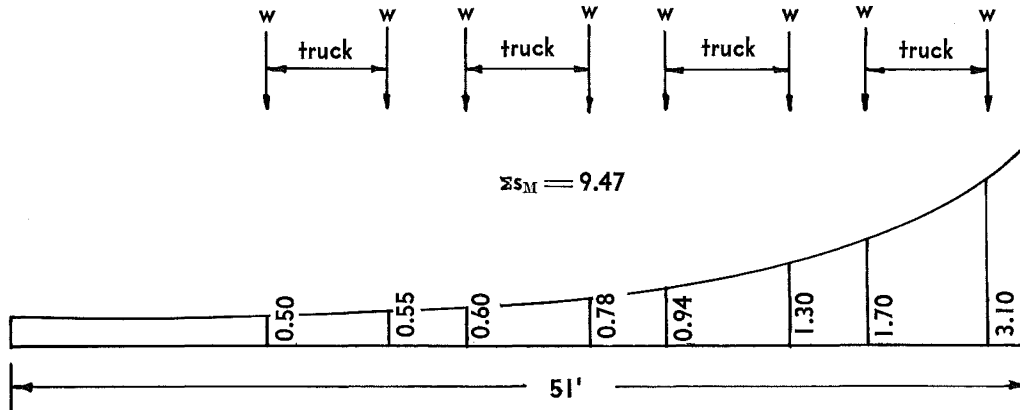
$$\frac{\geq s_M}{m} = \frac{8.74}{17} = 0.514$$

Edge loading:

$$\frac{\geq s_M}{m} = \frac{9.47}{17} = 0.557$$

4. Analysis of a single beam

In this example the edge loading yields the maximum moment. Thus a single beam has to be loaded with as many wheel loads as the specifications prescribe, but each wheel load may be reduced by the factor 0.557.

43

G. NOTATIONS

a   Width of single beam

B   ½ width of bridge

EI_x Longitudinal bending stiffness

EI_y Lateral bending stiffness

F   Total post-tensioning force

h   Depth of single beam

I_y Lateral moment of inertia

L   Length of bridge

m   Number of individual beams

M_x Longitudinal bending moment

M_y Lateral bending moment

M_{yx} Twisting moment

M_{xy} Twisting moment

n   Number of wheel loads over one cross-section

P   Applied concentrated load (P_e=edge, P_c=center)

Q_x Longitudinal shear force

Q_y Lateral shear force

s   Denotes coefficient

w   Deflection

$\propto$ EI_y / EI_x

β Coefficient of torsional rigidity

FIGURES

TABLES

CORRECTIONS

Page 6, Fig. 2 top:
Bridge Cross-Section instead of Beam
Cross-Section.

Tables 1 and 2a-2f
Slip (1/1000") should be Slip (1/10000")

Page 29, Paragraph 6a:
should read:
The values of the coefficients for the meas-
ured deflections are presented in Tables
2a - 2f. The calculated longitudinal bend-
ing moments were found by . . .

Page 31:
Heading 7a: "the parameter" should read
"the parameter α ."

Fig. 25: Relationship between α and $\dfrac{F}{P_c}$

Fig. 26: Relationship between α and $\dfrac{F}{P_e}$

Page 42 bottom:
instead of "may not be read"
should be "may be read"

Page 43:
Figures should be in reversed sequence.